AD-A162 053 ALGORITHMS FOR THE REDUCTION OF WIND-TUNNEL DATA DERIVED FROM STRAIN GAUGE FORCE BALANCES(U) AERONAUTICAL RESEARCH LABS MELBOURNE (AUSTRALIA) 1/1

UNCLASSIFIED B D FAIRLIE MAY 84 ARL/AERO-164 F/G 14/2 NL

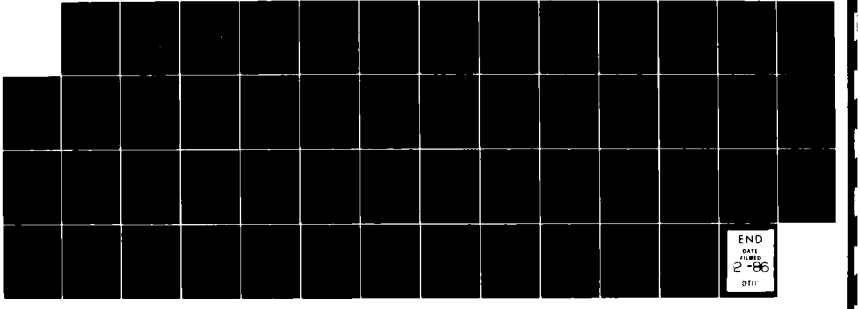

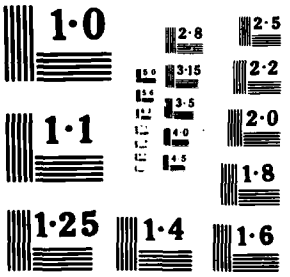
1·0
1·1
1·25
2·8
3·15
3·5
4·0
4·5
1·4
2·5
2·2
2·0
1·8
1·6

ARL/AERO-R-164

AR-004-017

(12)

AD-A162 053

DEPARTMENT OF DEFENCE

DEFENCE SCIENCE AND TECHNOLOGY ORGANISATION

AERONAUTICAL RESEARCH LABORATORIES

MELBOURNE, VICTORIA

AERODYNAMICS REPORT 164

ALGORITHMS FOR THE REDUCTION OF WIND-TUNNEL DATA DERIVED FROM STRAIN GAUGE FORCE BALANCES

DTIC ELECTE DEC 6 1985 S D B

by

B. D. FAIRLIE

THE UNITED STATES NATIONAL TECHNICAL INFORMATION SERVICE IS AUTHORISED TO REPRODUCE AND SELL THIS REPORT

Approved for Public Release

DTIC FILE COPY

© COMMONWEALTH OF AUSTRALIA 1985

MAY 1984

85 12 2 146

AR-004-017

DEPARTMENT OF DEFENCE
DEFENCE SCIENCE AND TECHNOLOGY ORGANISATION
AERONAUTICAL RESEARCH LABORATORIES

AERODYNAMICS REPORT 164

ALGORITHMS FOR THE REDUCTION OF WIND-TUNNEL DATA DERIVED FROM STRAIN GAUGE FORCE BALANCES

by

B. D. FAIRLIE

DTIC
ELECTE
DEC 6 1985
S D
B

SUMMARY

Algorithms and procedures are presented for the reduction of force and moment data derived from wind-tunnel models supported by internal strain-gauge balances. The algorithms are developed in their most general forms, suitable for implementation on the new generation of powerful minicomputers currently being included in wind-tunnel data acquisition systems. Although the emphasis of the report is on the treatment of data derived from sting mounted strain-gauge force balances, the analysis is applicable, with only minor modifications, to data derived from modern load-cell based external force balances.

© COMMONWEALTH OF AUSTRALIA, 1985

POSTAL ADDRESS: Director, Aeronautical Research Laboratories,
Box 4331, P.O., Melbourne, Victoria 3001, Australia

CONTENTS

QUALITY INSPECTED 3

Avail

Dist

A-1

NOTATION

A	arbitrary vector
A	coefficient in transformation matrix $\lambda_{BB'}$
a	speed of sound
a	slot width
B	coefficient of transformation matrix $\lambda_{BB'}$
B	tunnel width
b	span
C	cross wind force
C	tunnel cross-sectional area
C_{ij}	sensitivity and interaction coefficient
$[C]$, $[C1]$, $[C2]$	sensitivity and interaction coefficient matrices
c	chord
D	drag force
$[D]$	diagonal matrix of primary sensitivity coefficients
d	control surface length scale
d	slot spacing
F	slot parameter
F	arbitrary force vector
f	fuselage finesc ratio
G	arbitrary couple
g	unit gravity vector
H	total pressure
H	tunnel height
H	total applied load
H_{ij}	component load

h	hinge moment
$[J]$	critical stress coefficient matrix
$[K]$	deflection matrix
k_i	element of $[K]$
L	lift force
l	rolling moment
l	length
M	Mach number
m	pitching moment
n	yawing moment
P	static pressure
P	porosity parameter
q	dynamic pressure ($= 1/2\rho V^2$)
R	strain gauge amplifier output
Re	Reynolds number
S	reference area
T	interference parameter
t	aerofoil thickness
u	velocity component
V	volume
$\mathbf{V}$	free stream velocity
v	velocity component
W	weight
w	velocity component
X	axial force
$[X]$, $[X1]$, $[X2]$	normalized interaction coefficient matrices
x	ordinate
Y	side force
y	ordinate

Z	normal force
z	ordinate
α	angle of incidence
β	angle of sideslip
β	Prandtl–Glauert compressibility parameter $= (1-M^2)^{\frac{1}{2}}$
γ	ratio of specific heats
δ	interference parameter
Δ	approximation to applied load **H**
ϵ	blockage factor
$\zeta_{1,2,3}$	accelerometer outputs
η	angular deflection
θ	pitch angle
λ	direction cosine matrix
μ	dynamic viscosity
ν	kinematic viscosity
$\xi_{1,2,3}$	angular rotation from balance to body axes
ρ	density
σ	balance critical stress
τ	interference parameter
υ	angular deflection
ϕ	roll angle
χ	angular deflection
ψ	yaw angle
$\omega_{1,2,3}$	angular rotation from accelerometer to body axes

Superscripts

*	non-linear vector or matrix of component loads
$[\ ]^T$	transpose of a matrix
$[\ ]^{-1}$	matrix inverse

Subscripts

A	accelerometer axes
B	body axes
B'	balance axes
b	base
b	body or fuselage
f	free air
H	hinge
m	*missile* axes
o	wind off value
R	rig or indicated value
S	stability axes
s	sine definition
s	solid body
T	tailplane
T	tunnel axes
t	tangent definition
t	uncorrected (i.e. measured) values
w	wind axes
W	wake

Note—Symbols designating forces and moments—X, Y, Z, l, m, n, D, C, L and h are also used as subscripts when forces and moments are expressed in coefficient form, e.g. C_L = lift coefficient.

1. INTRODUCTION

An operating wind tunnel is potentially capable of generating large quantities of raw data in a very short period. The ever increasing cost of staffing, maintaining and running major wind tunnels has generated a strong economic inducement to increase wind tunnel efficiency by speeding up the acquisition and recording of test data. One common method of achieving this aim has been to use computer based data acquisition and processing systems. From the time when general purpose digital computers first became available, they have been used in such systems. Early (late 1950's and early 1960's) computer based systems made use of off-line general purpose machines.[1] These machines were generally remote from the wind tunnel, data being recorded at the wind tunnel site (usually with relatively slow paper tape or card punches) and transported to the central machine for later processing. With such systems, results were often not available for hours or even days after the test.

The advent of the minicomputer in the mid-1960's led to the development of dedicated wind tunnel computer systems. Processed test results were then available immediately following the test, and in some cases in real-time (or nearly so) during the test. Connection of the computer directly to the wind tunnel measuring instruments (often using parallel data transfers) also allowed a significant increase in the rate at which data could be recorded and processed. Large increases in tunnel efficiency resulted from the increased data collection rate, but more importantly from the new-found ability to detect and correct erroneous data while a test was in progress. However, early dedicated minicomputer systems suffered from slow execution speeds and from severely limited memory capacity. This led to the need to minimize the size of data reduction programs and sometimes to undesirable limitations on generality or compromises on overall accuracy.

Developments in the computer technology since the 1960's have seen the cost effectiveness of minicomputers increase by factors of up to 50. In current installations it is not uncommon for a dedicated wind tunnel minicomputer to support 4 Megabytes of memory and to operate at speeds of one million operations per second or more. This class of machine, which is significantly more powerful than even the largest of the machines available in the 1960's, allows a completely general approach to be taken when implementing data acquisition and processing algorithms. No longer is there any excuse for computer generated compromises on accuracy. These new machines also allow system designers to explore quite new approaches to wind tunnel data acquisition. For example, the high speeds of these machines permit a much greater degree of real time data monitoring and active model attitude control, leading to the feasibility of completely new methods of acquiring data, such as constant parameter testing techniques.[2] Indeed, it is now feasible for a wind tunnel test to be conducted completely under computer control.

The purpose of this report is to set out, in the most general way, the algorithms and procedures for the acquisition and processing of wind tunnel data derived from internal strain gauge force balances. Although some material has been directly reproduced from other sources, it was considered worthwhile to bring together, in their most general forms, all the algorithms required. With the more powerful minicomputers now in use in wind tunnels, such an approach may be implemented almost directly. The development assumes that the major source of data is the familiar internal, sting mounted strain gauge balance, but the analysis could be applied, with only minor modifications, to data acquired from modern load-cell based external balances.

The report is split into two parts. The first part, consisting of Sections 2 and 3, presents formal definitions of the axes systems in common use, and the sets of angles which relate one axes system with another. The use of these angles to transform data from one axes system to another are also included. The second part, making up the remainder of the report, sets out the procedures and algorithms required to convert raw wind tunnel data to a form suitable for use

by a customer. The three sections which make up this part of the report, divide the overall process into three logically separate stages:

(i) Calculation of the aerodynamic loads acting on the model. This involves the conversion of strain gauge bridge outputs to applied loads, correction of these applied loads for the effects of model and balance mass, transformation to body axes, and formation of non-dimensional coefficients. Allowance must also be made for the effects of base pressures.

(ii) Determination of the attitude of the model and hence the orientation of the body axes system with respect to the relative wind vector.

(iii) Application of corrections for the effects of wind tunnel wall interference (carried out in the wind axes system) and finally the transformation of data to the axes systems required by the customer.

Although the overall approach presented in this report is followed by the computer based data acquisition system recently installed in the A.R.L. low-speed wind tunnel,[3] this system does not as yet fully implement all of the procedures. It is hoped that this full implementation can be achieved in the near future.

2. SYSTEMS OF AXES

When formulating and solving problems involving internal strain gauge balances and their mounting systems, a number of frames of reference (systems of axes) must be considered. Each of the axes systems considered here is an orthogonal right-handed system. In all, six axes systems will be considered. This is not an exhaustive set, the choice being based on convenience, usefulness, and to some extent personal preference.

Tunnel Axes—x_T, y_T, z_T: with the x_T axis coincident with, and in the same direction as the relative free-stream wind vector (usually horizontal), and the y_T axis perpendicular to the longitudinal tunnel axis and horizontal, positive to the right when looking in the direction of x_T.

Tunnel axes are fixed in the wind tunnel and serve as the locally applicable earth-fixed (and inertial) reference frame. Tunnel axes are rarely used to express aerodynamic loads.

Wind Axes—x_W, y_W, z_W: with the x_W axis parallel to the relative wind vector, positive into the wind, and the z_W axis in the plane of symmetry of the model if it has one, otherwise arbitrary.

Wind axes are the traditional frame of reference for the expression of aerodynamic coefficients and the calculation of wind tunnel wall interference (although tunnel axes may be preferable for the latter if the tunnel is of non-circular cross-section and the model plane of symmetry is not parallel to one of the tunnel axes of symmetry). Note that tunnel axes and wind axes differ by at most an angle of roll. If the model does not have a plane of symmetry, it is customary to take the Y_W axis to be horizontal when the model is in its defined zero roll orientation.

Body Axes—x_B, y_B, z_B: with the x_B axis along the model longitudinal axis, positive forward, and the z_B axis in the model plane of symmetry, positive "downwards".

Body axes remain fixed in the model and remain related to it via reference planes, e.g. the chord or fuselage reference line, plane of symmetry and plane of the wings for an aircraft model. For models without planes of symmetry, e.g. missiles, the y_B and z_B axes are usually defined to be in some convenient mutually perpendicular directions.

Stability Axes.—x_S, y_S, z_S: with the x_S axis parallel to the projection of the relative wind vector on the plane containing the x_B and y_B axes, positive forward, and the y_S axis coincident with and in the same direction as the y_B axis.

Stability axes are a special set of body axes of considerable importance in the study of flight dynamics. The stability axes yaw with the model but do not pitch.

Missile Axes.—x_m, y_m, z_m: with the x_m axis coincidant with and in the same direction as the x_B axis, and the y_m axis coincident with and in the same direction as the y_B axis with the yaw and roll angles zero.

Missile axes, also known as "non-rolling body axes", are frequently used in missile flight dynamics.

The origins for all of the above axes systems are usually assumed to coincide when the model is in its reference (zero pitch, yaw and roll) condition. The position of the origin in this reference condition is normally chosen to be the location of the full-scale aircraft centre of gravity in the model, but may be any convenient reference position. Depending on the details of the equipment used to change model attitude, the origins of the various axes systems may no longer coincide at finite model attitudes.

In general, the moment centre used for the calibration of a strain gauge balance will not coincide with the chosen origin for the body axes system. In order to allow use of balance calibrations carried out in arbitrary axes systems, it is useful to define a further set of axes – balance axes.

Balance Axes.—x'_B, y'_B, z'_B: with the x'_B axis parallel to the longitudinal axis of the balance or other axis used for the x-direction during calibration, positive "forwards", and the z'_B axis similarly defined, positive "downwards".

The balance axes system is equivalent to the body axes system, but with the origin at the moment centre assumed during balance calibration and with the axes in those directions used during balance calibration. Note that it is usual to assume that the balance is infinitely stiff between the "model end" and the moment centre, i.e. the origin and direction of the balance axes are fixed with respect to the model end of the balance.

For all the above axes systems, the components of the net force **F** acting through the origin are defined to be X, Y and Z in the x, y and z directions respectively (with suitable subscripts added to indicate the particular axes system in use). For compatibility with aircraft stability theory, three additional forces L (lift), D (drag) and C (cross-wind force) are defined in the wind axes system (and occasionally in the stability axes system). These additional forces are related to X, Y and Z by

$$L = -Z_W$$

$$D = -X_W$$

$$C = -Y_W$$

The components of the net couple **G** acting about the origin are defined as l, m and n.

Note that in the remainder of this report, the subscript B (body axes) will be dropped where there is no possibility of confusion.

In the body axes system, the components of the relative wind vector **V** in the x_B, y_B and z_B directions are defined to be u, v and w respectively.

3. DEFINITIONS OF ANGLES

Reduction of wind-tunnel data involves the use of several frequently used angles. These angles fall into two categories: aerodynamic angles and positioning or orientation angles.

3.1 Aerodynamic Angles

The orientation of the model with respect to the relative wind vector **V** can be defined in terms of either the three orthogonal components of **V** in the body-axis system (u, v, w), or more conveniently, by the magnitude of **V** and two suitably defined angles. These two angles are known as the angles of incidence α, and sideslip β. Currently there are two alternate definitions in use for α and β—the tangent definitions and the sine definitions—and there is a need for precision in stating which definition is in force.

Tangent Definitions

α_t is the angle between the model x_B-axis and the projection of the wind vector on the x_B, z_B plane, i.e.

$$\tan \alpha_t = \frac{w}{u}$$

β_t is the angle between the model x_B-axis and the projection of the wind vector on the x_B, y_B plane, i.e.

$$\tan \beta_t = \frac{v}{u}$$

Sine Definitions

α_s is the angle between the wind vector and its projection on the model x_B, y_B plane, i.e.

$$\sin \alpha_s = \frac{w}{V}$$

β_s is the angle between the wind vector and its projection on the model x_B, z_B plane, i.e.

$$\sin \beta_s = \frac{v}{V}$$

The merits of the two sets of angles thus defined (and combinations thereof) have been considered by Warren.[4] As he points out, the traditional approach to aircraft stability and control was to use the wind axes system, and to assume that squares of component velocities in the y_B and z_B directions (v^2, w^2) could be neglected, and that the x-component of velocity u was equivalent to the total velocity V. Under these conditions, tangent and sine definitions are equivalent. Since that time, testing of missiles and modern aircraft at large combined values of α and β (i.e. large values of v and w) has invalidated these assumptions and hence the two definitions must be differentiated.

Workers in the missile flight dynamics field prefer to use the same definition of both incidence and sideslip to preserve the inherent symmetry of the missile configuration. However the choice of either the tangent or sine definition is rather arbitrary, although there is some argument for using the tangent definition. In the aircraft field, the increasing use of stability axes in stability and control theory leads to the preference for the tangent definition of incidence and the sine definition of sideslip. This choice (α_t, β_s) also leads to particularly simple definitions in terms of the orientation angles for the traditional yaw/pitch rig commonly used in low-speed wind tunnels (see Appendix A).

For the remainder of this report relationships will be developed only for the combination α_t, β_s and their subscripts will be dropped where there is no possibility for confusion. However, relationships for other combinations will be presented in the Appendices so that that combination best suited to a particular test (or customer) may be used.

3.2 Orientation Angles

The orientation of one set of axes relative to any other set can be given by three angles, which are the consecutive rotations about the axes z, y, x in that order that carry one set of axes into coincidence with the other. This is a special case of "Euler Angles". In wind tunnel testing the Euler angles of interest are those that rotate the tunnel-axes system x_T, y_T, z_T into coincidence with the body-axis system, and the angles are ψ, θ and ϕ. Referring to Figure 1, these angles may be defined as:

ψ—the yaw angle—rotating the tunnel-axes system about oz_T to give the axes x_2, y_2, z_2.

θ—the pitch angle—rotating the x_2, y_2, z_2 system about oy_2 to give the axes x_3, y_3, z_3.

ϕ—the roll angle—rotating the x_3, y_3, z_3 system about ox_3 to give the body-axes system x_B, y_B, z_B.

The positive directions for ψ, θ and ϕ obey the normal right-hand screw rule about the relevant axes.

It must be noted that the sequence in which the rotations (ψ, θ, ϕ) are taken is important. If the sequence is changed, the orientation of the body-axes system with respect to the (fixed) tunnel-axes system (and hence the values of α and β) will also change.

To avoid ambiguities which can otherwise result in the set of angles (ψ, θ, ϕ) the ranges are limited to

$$-\pi \leqslant \psi \leqslant \pi \quad \text{or} \quad 0 \leqslant \psi \leqslant 2\pi$$

$$\pi/2 \leqslant \theta \leqslant \pi 2$$

$$\pi \leqslant \phi \leqslant \pi \quad \text{or} \quad 0 \leqslant \phi \leqslant 2\pi$$

The Euler angles are then unique for most model orientations and give aerodynamic angles in the ranges

$$\pi \leqslant \alpha \leqslant \pi$$

and

$$\pi \leqslant \beta \leqslant \pi$$

3.3 Relationships Between Aerodynamic and Orientation Angles

In the wind tunnel the model, and hence the body-axes system can be rotated through the Euler angles (ψ, θ, ϕ), and this rotation causes the aerodynamic angles α and β to exist. As pointed out by Warren,[4] perhaps the clearest way of showing the angles of incidence and sideslip that are produced by the rotation (ψ, θ, ϕ) is to visualize the trace of a point on the x_B-axis on the surface of a sphere whose centre is at the origin.

Figure 2 shows the general case. If P is the initial position of the point on the x_B-axis, the x_B, y_B plane being the horizontal plane WPE, and the x_B, z_B plane being the vertical plane NPS, rotating the model through an angle of yaw ψ moves P to P_1, the x_B, y_B plane remaining in WPP_1E and the x_B, z_B plane moving to NP_1S. Rotating through an angle of pitch θ moves P_1 to P_2, the x_B, y_B plane moving to $W_1P_2E_1$ while the x_B, z_B plane remains in NP_2P_1S. Finally rotating through an angle of roll ϕ does not change P_2, but the x_B, y_B plane moves to $W_2P_2E_2$ and the x_B, z_B plane to $P_2N_2S_2$. If PQ and PR are perpendicular to $N_2P_2S_2$ and $W_2P_2E_2$ respectively, then the definitions of the angles of sideslip and incidence are equivalent to arcs of great circles on the surface of the sphere as follows:

$$\alpha_1 = P_2Q$$

$$\beta_1 = P_2R$$

$$\alpha_s = PR$$

$$\beta_s = PQ$$

By the application of elementary spherical trigonometry it may be shown that

$$\sin \alpha_s = \cos \psi \sin \theta \cos \phi + \sin \psi \sin \phi \tag{3.1}$$

$$\sin \beta_s = \cos \psi \sin \theta \sin \phi - \sin \psi \cos \phi \tag{3.2}$$

$$\tan \alpha_1 = \tan \theta \cos \phi + \frac{\tan \psi \sin \phi}{\cos \theta} \tag{3.3}$$

$$\tan \beta_1 = \tan \theta \sin \phi - \frac{\tan \psi \cos \phi}{\cos \theta} \tag{3.4}$$

Special forms of the above equations applicable to particular cases, together with their forms in the presence of additional small deflections, are set out in Appendix A.

3.4 Transformations Between Systems of Axes

Consider two orthogonal right-handed systems of axes denoted x_1, x_2, x_3 and x_1', x_2', x_3'. The direction of the x_1', x_2', x_3' set of axes with respect to the x_1, x_2, x_3 set, may be expressed as a matrix of direction cosines.

$$[\lambda] \quad \begin{bmatrix} \lambda_{11} & \lambda_{12} & \lambda_{13} \\ \lambda_{21} & \lambda_{22} & \lambda_{23} \\ \lambda_{31} & \lambda_{32} & \lambda_{33} \end{bmatrix}$$

where λ_{pq} is the cosine of the angle between the x'_p and x_q axes.

Amongst the many useful properties of this matrix which may be derived,[5] those of interest in the present area are as follows:

(i) The inverse of the direction cosine matrix and its transpose are equal, i.e.

$$[\lambda]^{-1} = [\lambda]^T \tag{3.5}$$

(ii) Consider a vector **A**. The components of **A** in x_1', x_2', x_3', **A'** where

$$\mathbf{A}' = \begin{bmatrix} A_1' \\ A_2' \\ A_3' \end{bmatrix}$$

are related to its components in the x_1, x_2, x_3 system, **A**, via

$$\mathbf{A}' = [\lambda]\mathbf{A} \tag{3.6}$$

This transformation may be readily inverted using (3.1).

$$\begin{aligned} \mathbf{A} &= [\lambda]^{-1}\mathbf{A}' \\ &= [\lambda]^{T}\mathbf{A}' \end{aligned} \tag{3.7}$$

In the present context we are interested in the ability to express the model loads determined in one axes system in some other axes system. For example, the components of the model force vector **F** in the tunnel axes system ($\mathbf{F}_T$) may be obtained from its components in the body axes system ($\mathbf{F}_B$) from

$$\mathbf{F}_B = [\lambda]_{BT}\,\mathbf{F}_T \tag{3.8}$$

where $[\lambda]_{BT}$ is the matrix of direction cosines which relate the direction of the body axes system to the tunnel axes system. It may be shown that in terms of the Euler angles (ψ, θ, ϕ) which rotate the tunnel axes into the body axes, this matrix is given by

$$[\lambda]_{BT} = \begin{bmatrix} \cos\theta\cos\psi & \cos\theta\sin\psi & -\sin\theta \\ \sin\phi\sin\theta\cos\psi - \cos\phi\sin\psi & \sin\phi\sin\theta\sin\psi + \cos\phi\cos\psi & \sin\phi\cos\theta \\ \cos\phi\sin\theta\cos\psi + \sin\phi\sin\psi & \cos\phi\sin\theta\sin\psi - \sin\phi\cos\psi & \cos\phi\cos\theta \end{bmatrix} \tag{3.9}$$

The inverse transformation—from tunnel axes to body axes is then given by

$$\begin{aligned} \mathbf{F}_T &= [\lambda]_{TB}\,\mathbf{F}_B \\ &= [\lambda]_{BT}^{-1}\,\mathbf{F}_B \\ &= [\lambda]_{BT}^{T}\,\mathbf{F}_B \end{aligned} \tag{3.10}$$

Appendix B presents transformation matrices for the transformation of vector components between the more often utilized sets of axes—body, stability and wind-axes. The matrices are presented for all useful combinations of the aerodynamic angles α_s, β_s, α_t and β_t.

4. DETERMINATION OF AERODYNAMIC LOADS ON THE MODEL

This section addresses the problem of the determination of the aerodynamic loading applied to a model from the outputs of amplifiers connected to each strain gauge bridge output. It

will be assumed in what follows that the linearity of the strain gauge bridge amplifiers is sufficient for them not to effect the relationship between applied load and amplifier output, and hence that a balance calibration is independent of the particular set of amplifiers in use (except possibly for an adjustment for amplifier gain). In practice, this assumption is valid for the amplifiers in use at ARL, the newer types[6] being an order of magnitude more linear (0·01 %) than the expected accuracy of a balance calibration (0·1 %).

The determination of aerodynamic loads may be considered in several stages. Firstly, experience has shown that for the newer amplifiers, although the overall gain of the bridge/amplifier system is extremely stable, the system is susceptible to zero drift which must be corrected. This zero drift has several sources, the major contribution being the effect of temperature on the strain gauge bridge itself (both bulk temperature and temperature gradients). For some older amplifiers, a correction for amplifier gain drift must also be made.

Secondly, the gross loads acting on the model must be calculated by the solution of the balance equations for a six-component balance or by the application of simple linear calibration to hinge-moment measuring bridges. Finally the model weight tares must be calculated and subtracted from the gross loads to give the net aerodynamic loads acting on the model.

The components of aerodynamic loads thus calculated will be expressed in the balance axes system. Before being useful for further analysis, the load components must be converted to dimensionless coefficient form, and the influence of stings on pressures acting on blunt bases taken into account. Finally the corrected balance axes coefficients must be transformed to the body axes system, taking into account both the angular relationships between the two axes systems and any offset between the balance moment centre and the origin of the body axes system.

4.1 Corrections to Balance Outputs

For a model mounted on a six-component strain gauge balance, the outputs of the balance will be presented as six output channel readings R_i' $i = 1, 6$. If hinge moments are being measured there will be additional outputs R_H' from the moment measuring strain-gauge bridges—one for each hinge moment. In general, these outputs will not be zero in the wind-off condition and this value (the "zero" reading) must be subtracted from the wind-on outputs—

$$\left.\begin{aligned} R_i &= R_i' - R_{i0} \\ \text{and} \\ R_H &= R_H' - R_{H0}' \end{aligned}\right\} \qquad (4.1)$$

It is also desirable to correct the raw balance outputs for any drift in these "zero" readings *during a run*. This may be achieved if a wind-off "zero" reading is recorded at the same attitude at the beginning and end of each wind-tunnel run and the wind-on outputs corrected via

$$\left.\begin{aligned} R_i &= R_i' - \left[\frac{(R_{i0}')_{\text{beginning}} + (R_{i0}')_{\text{end}}}{2}\right] \\ \text{and} \\ R_H &= R_H' - \left[\frac{(R_{H0}')_{\text{beginning}} + (R_{H0}')_{\text{end}}}{2}\right] \end{aligned}\right\} \qquad (4.2)$$

Obviously it is not possible to apply such a correction scheme until the run has been completed and the wind-off "zero" reading recorded. For data presentation in "real-time" (i.e. during a run), the correction scheme of equation (4.1) must be used.

For strain-gauge readout equipment having variable sensitivity and where a "calibration" of the sensitivity setting is possible, a scheme analogous to that of (4.2) can be applied to beginning and end of run "calibration "readings.

4.2 Reduction of Balance Outputs to Gross Forces and Moments

Although the designer of a strain-gauge balance attempts to make each output sensitive to only one load component, it is not possible to eliminate entirely interactions due to other components. In many cases, especially where the balance design loads are large for the size of the balance, it is necessary to take into account the presence of non-linear interactions in addition to the usual linear interactions.

In general the outputs of the strain gauge bridge for each component are, due to these interactions, functions of all component loads. The reading for the ith balance component is usually expressed as a polynominal function of the applied loads, and for well designed balances it is generally found that terms of third and higher degree in load components are negligible, while the coefficients of second degree terms are small, but possibly significant. Hence each component output may be represented to sufficient accuracy by a second order *polynomial* of the form

$$\left.\begin{aligned} R_i = {} & C_{i,1}H_1 + C_{i,2}H_2 + \ldots\ldots + C_{i,6}H_6 \\ & + C_{i,11}H_1^2 + C_{i,22}H_2^2 + \ldots\ldots + C_{i,66}H_6^2 \\ & + C_{i,12}H_1F_2 + C_{i,13}H_1H_3 + \ldots\ldots + C_{i,56}H_5H_6 \end{aligned}\right\} \qquad (4.3)$$

Where the C's are the *calibration coefficients determined* during balance calibration and H_i are the component loads. The calibration coefficients may be classified as follows:

(*a*) "linear", e.g. $C_{i,j}$, $j = 1,6$

(*b*) "load squared", e.g. $C_{i,jj}$, $j = 1,6$

(*c*) "load cross product", e.g. $C_{i,jk}$, $j = 1,5$, $k = j+1,6$

It follows that for each component there are 27 calibration coefficients, giving a total of 162 for a six-component balance.

The set of six simultaneous equations represented by (4.3) to describe balance output are most conveniently represented in matrix form, with the calibration matrix partitioned into "linear" and "non-linear" sub-matrices:

$$\mathbf{R} = [C1]\,\mathbf{H} + [C2]\,\mathbf{H}^* \qquad (4.4)$$

where

R is the vector of component outputs

[C1] is the matrix of linear calibration coefficients, $C_{i,j}$

[C2] is the matrix of non-linear calibration coefficients, $C_{i,jj}$ and $C_{i,jk}$

H is the vector of component loads

H* is the vector of squares and cross products of component loads.

It is useful to "normalize" the linear and non-linear calibration matrices [C1] and [C2] by premultiplying each by a diagonal matrix [D] composed of the diagonal elements of the linear calibration matrix [C1] giving

$$\left.\begin{aligned} [X1] &= [D][C1] \\ [X2] &= [D][C2] \end{aligned}\right\} \qquad (4.5)$$

This has the effect of allowing the elements of [X1] and [X2] to have universal application while those of [D] are dependent on the particular readout system in use. A factor for converting from one readout system to another of the same type can then be simply applied to the "primary sensitivity" matrix [D].

The procedure for determining the component load vector from the component outputs via equation (4.4) has been described previously[7,8,9] but is included here for completeness. Pre-multiplication of both sides of (4.4) by [D] yields

$$[D]\,\mathbf{R} = [D][C1]\,\mathbf{H} + [D][C2]\,\mathbf{H}^*$$

or

$$\mathbf{H}' = [X1]\,\mathbf{H} + [X2]\,\mathbf{H}^*$$

where $\mathbf{H}'$ is a vector of approximate component loads ignoring all (both linear and non-linear) interactions. Solving for $\mathbf{H}$ gives

$$\mathbf{H} = [X1]^{-1}\mathbf{H}' - [X1]^{-1}[X2]\,\mathbf{H}^* \qquad (4.6)$$

If there are no non-linear terms in the balance calibration then $[X2] = 0$ and $\mathbf{H}$ is given by the explicit solution

$$\mathbf{H} = [X1]^{-1}\mathbf{H}' \qquad (4.7)$$

If however non-linear terms are significant, then (4.6) must be solved by an iterative method. A first approximation to $\mathbf{H}$ may be obtained by ignoring the non-linear terms, i.e. from (4.7)

$$\mathbf{H}_1 = [X1]^{-1}\mathbf{H}'$$

and this approximation may be used to obtain a first approximation of the non-linear term (Δ_1) thus

$$\Delta_1 = [X1]^{-1}[X2]\,\mathbf{H}_1^*$$

where the elements of the vector $\mathbf{H}_1^*$ are composed of the squares and cross-products of the elements of the approximate vector $\mathbf{H}_1$.

A second approximation $\mathbf{H}_2$ is then obtained from

$$\mathbf{H}_2 = \mathbf{H}_1 - \Delta_1$$

This procedure may be generalised into an iterative scheme where an approximation to the non-linear terms

$$\Delta_n = [X1]^{-1}[X2]\,\mathbf{H}_n^* \qquad (4.8A)$$

is used to produce a new approximation to the component loads **F** from

$$\mathbf{H}_n = \mathbf{H}_1 - \mathbf{\Delta}_{(n-1)} \tag{4.8B}$$

where n is iteration number.

The convergence of this scheme has been investigated in Reference 7, but for typical balances with small non-linear effects, convergence is usually very rapid (two to three cycles).

The output of hinge moment measuring bridges can usually be represented to sufficient accuracy by a linear calibration of the form

$$R_H = C_H H_H \tag{4.9}$$

and determination of the applied load H_H from the output R_H is trivial.

4.3 Tare Weight Corrections

For a model mounted on an internal strain-gauge balance, distinction must be made between the part of the applied loads determined from (4.8) which is due to the wind, and that due to a change in model attitude. Due to the finite weight of a model, all strain gauge balance outputs will include the combined effect. However, since the attitude of the model with respect to horizontal is known or can be determined, the balance loads due to the weight components of the model can be calculated. The change in weight components due to the change in attitude from the wind-off "zero" condition to the wind-on measurement condition may then be calculated and deducted from the measured (combined) values to give the portion due to the wind alone.

The distribution of the model weight "tares" among the balance components is a function of the magnitude and centre of gravity position of the "metric mass" and the balance orientation with respect to the gravity vector. The presence of terms of other than first degree in the balance calibration matrix introduces a further difficulty when determining tares. This is the problem of defining what the true "zero" of the load scale should be. For anything but a linear calibration, the use of one "zero" for calibration of the balance, and others for load measurement will give rise to errors. To avoid this problem the concept of an "absolute zero load" or "bouyant" condition, first introduced by Galway,[9] will be used when calculating the tare components. This tare condition is, by definition independent of the balance orientation and the magnitude and centre of gravity position of the metric mass. All incremental measurements relative to this "bouyant" tare condition will then be proportional to load on an absolute scale.

When using the concept of "bouyant" tares, it is important to define exactly what is meant by the "metric mass" and to carefully distinguish between the "metric mass" and the weight of the model. The "metric mass" may be defined as all parts of the model/balance system as a whole, whose weight results in outputs on any balance component, the magnitude and distribution of which depend on the orientation of the model/balance system relative to the gravity vector. It is probable that, due to the construction of the balance and the placement of individual strain gauge bridges, different components will sense different "metric mass" contributions from different parts of the balance, and hence different total tare weights and centre of gravity locations.

The problem of determining the components of measured outputs which are due to the wind is therefore reduced to determining the "bouyant" condition for the strain gauge balance. The method used here is one in which the bouyant condition for each balance component is derived from the wind-off outputs from a series of distinct model/balance orientations. It is therefore unnecessary to determine the model weight and centre of gravity location by separate means.

Consider first the loads seen by each component of the balance due to the weight of the metric mass. For all types of model support, the only angular motions of the model/balance

with respect to the gravity vector are pitch and roll. Hence the loads due to the weight of the metric mass will be given by

$$\left.\begin{aligned} F_X &= -W_X \sin\theta \\ F_Y &= W_Y \cos\theta \sin\phi \\ F_Z &= W_Z \cos\theta \cos\phi \\ G_l &= W_l(y_l \cos\theta \cos\phi - z_l \cos\theta \sin\phi) \\ G_m &= -W_m(z_m \sin\theta + x_m \cos\theta \cos\phi) \\ G_n &= W_n(x_n \cos\theta \sin\phi + y_n \sin\theta) \end{aligned}\right\} \quad (4.10)$$

where the W's are the components of the metric mass, and the x, y, z's are the locations (measured in the balance axes system) of the centres of gravity of these components, as seen by each balance component.

For a pitch-yaw type of model support, where the roll angle ϕ is constrained to be zero, these loads reduce to

$$\left.\begin{aligned} F_X &= -W_X \sin\theta \\ F_Y &= 0 \\ F_Z &= W_Z \cos\theta \\ G_l &= W_l\, y_l \cos\theta \\ G_m &= -W_m\,(z_m \sin\theta + x_m \cos\theta) \\ G_n &= W_n\, y_n \sin\theta \end{aligned}\right\} \quad (4.11)$$

Initially, with the balance and model set (with the wind-off) at some attitude θ_o, ϕ_o (usually, but not necessarily $\theta_o = 0^\circ$, $\phi_o = 0^\circ$), the output of each component is recorded as a "zero" reading, $(R_i)_0$. This reading is not the output the balance would have at that attitude at "bouyant" conditions, but it may be considered as an approximation of the bouyant condition with all tare components of the metric mass assumed to be zero. The balance and model are then moved to a different attitude (still with the wind-off) where the output of each component is $(R_i)_1$. The change in output

$$\Delta R_i = (R_i)_1 - (R_i)_0$$

may then be used to calculate the change in applied load ΔH_i corresponding to the change in attitude (using the calibration matrix and the iterative scheme (4.8)). This calculated change in applied load may be used with the equations of (4.10) or (4.11) to obtain an approximation to the components of the metric mass. For example, from (4.11) the change in the x-component load is given by

$$\Delta F_X = -W_X (\sin\theta - \sin\theta_o) \quad (4.12)$$

and hence W_X may be determined.

These approximate components of the metric mass may in turn be used to determine a better approximation R_i^* to the "bouyant" outputs of each balance component. Returning to

the x-component example, having computed W_X it may be used to calculate the tare load component at $\theta = \theta_o$ using (4.10) thus

$$F_X^* = W_X \sin \theta_o$$

and once all the H_i^* have been determined, the balance calibration matrix can be used to give the R_i^* using (4.4). The change in output ΔR_i for the change in attitude is then recalculated but now including the approximation to the "bouyant" tare reading

$$\Delta R_i = (R_i)_i - (R_i)_0 - R_i^* \tag{4.13}$$

which may be used to calculate a more accurate estimate of the components of the metric mass. The whole process is repeated until successive approximations to the metric mass components agree to within some tolerance.

It should be noted that the above procedure does not yield explicit estimates of the magnitudes of all the metric mass components or of their centre of gravity locations, but rather estimates of the values of their products (e.g. $W_m z_m$). However, since these products are in fact the values required in the application of the overall scheme, this does not represent a problem.

In principle, only two model/balance attitudes are necessary to determine the metric mass components. In practice however, it is desirable to make use of many attitudes to increase the accuracy of the process. The approach adopted here is to use the balance outputs from N distinct attitudes and then to represent equations such as (4.12) as least squares linear approximations. Statistical methods may then be used to calculate standard errors of estimate for each component to indicate the "goodness of fit".

Having determined the required values of the components of the metric mass, it remains to apply these and the concept of "bouyant" tares to the strain gauge balance outputs recorded during a wind tunnel run. The procedure is as follows:

(i) The loads applied to the balance by the metric mass at the attitude at which wind-off zeros are recorded may be computed from equation (4.10) or (4.11).

(ii) The readings of the six balance outputs corresponding to these loads may be calculated from the balance calibration matrices and equation (4.4).

(iii) Subtracting these readings from the wind-off zero readings R_{i0}' gives a set of "bouyant" zero readings.

(iv) These bouyant zeros may then be used to correct wind-on outputs using equation (4.1) or (4.2).

(v) The resulting set of absolute readings may they be converted to a set of equivalent absolute loads using the iterative scheme of equation (4.8).

(vi) Finally the aerodynamic components of this set of loads is calculated by subtracting the tare loads due to the metric mass at each wind-on attitude computed from either (4.10) or (4.11).

It should be noted that if the balance calibration matrix contains only linear terms, i.e. $[C2]$ in equation (4.4) is zero, then the above procedure may be simplified. In this case it is sufficient to calculate the change in loads on the balance from the metric mass due to the change in attitude from the wind-off zero to the wind-on data point. This change in load is then deducted from the measured wind-on loads to give the portion due to the wind.

The output of hinge moment measuring bridges will also be affected by the "metric mass" of the corresponding control surfaces. For most conventional control surfaces it is generally found that the effects of the metric mass, when compared to the required accuracy of measurement of hinge moments, are small enough to be ignored. In practice the wind-off outputs of

hinge moment measuring bridges should be observed over the complete range of attitudes to be tested. If the magnitude of the tare effects is greater than allowed by the desired accuracy of measurement, an analysis similar to that described above may be applied to determine the components of the metric mass and hence to separate tare and wind induced calibrations to hinge moment. Since hinge moment calibrations will generally be linear (e.g. equation (4.9)), the simplifications of the previous paragraph may be utilized. Equations similar to (4.10) or (4.11) giving the tare contribution to hinge moment as a function of attitude (in this case including the deflection of the control surface itself) may be formulated. Special attention should be paid to correctly accounting for sign conventions for both hinge moment and control deflection and the effect of hinge orientation with respect to the overall model balance axes (e.g. a flap or aileron on the swept trailing edge of a wing or a model mounted on a pitch/roll support deserves careful attention).

4.4 Balance Safe Loads

As described in the previous section, the use of the concept of "bouyant" tares allows the calculation of the absolute loads, i.e. the total loads resulting from all external fields, acting on the balance. Such absolute loads are exactly those required for checking that the loading state of the balance is such that maximum stress levels remain within the safe operating envelope. Traditionally, it has been the practice to define a maximum value for each of the six components applied to the balance, independent of the magnitudes of the other five. For most practical balances this will be a very conservative approach since the maximum values are usually derived on the basis that some or all of the components are at their maximum values simultaneously. An approach which allows the more efficient use of the total balance capacity is to check that for each set of applied loads the maximum stresses remain within safe limits. For modern balances for which no on-balance summing of bridge outputs is used, the most efficient approach is to calculate a set of maximum stresses from the absolute readings produced by the applied loads, i.e.

$$\boldsymbol{\sigma} = [J]\,\mathbf{R}^* \tag{4.14}$$

where $\boldsymbol{\sigma}$ is a vector of n elements corresponding to n critical stresses and $[J]$ is an $n \times 6$ matrix of coefficients determined for each particular balance design. $\boldsymbol{\sigma}$ is then compared with a set of n maximum allowable stresses.

This approach has the added advantage of avoiding the time-consuming iterative solution required to determine the absolute loads $\mathbf{H}$. The time saved is specially important when the state of the balance is to be checked at regular intervals in time rather than only at the times when data points are recorded.

4.5 Conversion to Coefficient Form

The aerodynamic loads acting on a model are usually expressed in the form of coefficients, forces being represented by

$$C_X = \frac{X}{qS}; \qquad C_Y = \frac{Y}{qS}; \qquad C_Z = \frac{Z}{qS} \tag{4.15}$$

and moments by

$$C_l = \frac{l}{qSb}; \qquad C_m = \frac{m}{qSc}; \qquad C_n = \frac{n}{qSb} \tag{4.16}$$

where q is the dynamic pressure, S reference area and b and c are reference lengths.

Dynamic pressure is calculated from the free stream static pressure (P) and the free stream total pressure (H) using the isentropic flow relationships

$$\frac{P}{H} = \left(1 + \frac{\gamma - 1}{2} M^2\right)^{-\gamma/(\gamma-1)}$$

giving

$$M^2 = \frac{2}{\gamma - 1}\left\{\left(\frac{P}{H}\right)^{(\gamma-1)/\gamma} - 1\right\}$$

and

$$q = \tfrac{1}{2}\rho V^2 = \tfrac{1}{2}\gamma P M^2$$

With $\gamma = 1{\cdot}4$ these equations become

$$M^2 = 5\left\{\left(\frac{P}{H}\right)^{-2/7} - 1\right\} \tag{4.17}$$

and

$$q = 0{\cdot}7\,PM^2 \tag{4.18}$$

It should be noted that the assumption (common in low speed wind tunnels) that

$$q = H - P$$

should be avoided in all wind tunnel testing. The error in this assumption amounts to $0{\cdot}5\%$ at $M = 0{\cdot}14$ ($V \approx 50$ ms^{-1}) rising to more than 2% at $M = 0{\cdot}3$ ($V \approx 100$ ms^{-1}).

For many tests in which the model is mounted via a rear sting, the pressure on the blunt base and hence the axial force acting on the model is influenced to a large extent by the sting. For tests where the sting enters the model by way of a jet engine exhaust duct, this problem may be overcome by correcting the axial force so that it corresponds to the zero base drag condition. To obtain flight values of axial force, the engine thrust coefficient is then added to this corrected axial force to give the total axial force. For models without jet engine exhausts, the problem of obtaining accurate measurements of base drag is much more difficult. In these cases the base geometry has probably been grossly distorted to allow entry of the sting. The base pressure will also be strongly affected by the presence of the sting and by the condition of the model boundary layer. The only practical methods for estimating base drag are to do a separate series of tests with the model mounted in some other manner, or to use purely empirical methods. In either case, results from sting supported tests should be corrected to the zero base drag condition to provide a rational starting point.

Hence it is desirable that all tests of sting mounted models should include a correction of axial force to the zero base drag condition. Given the pressure in the model cavity (P_b) and the area of the base "opening" (S_b), a base force coefficient may be defined by

$$C_{Xb} = \frac{(P_b - P)S_b}{qS} \tag{4.19}$$

where S is the reference area used to non-dimensionalize axial force coefficient. Axial force coefficient corrected to zero base drag is then given by

$$C_X = C_{X'} - C_{Xb} \tag{4.20}$$

where C_X' is the axial force coefficient measured by the balance.

The above analysis is only valid for cases in which the base area is normal to the balance axes x-axis, i.e. perpendicular to x_B', and the centroid of the base area is on the x_B' axis. These conditions are often satisfied in practical models (at least to a significant level of approximation). However, in the general case, base force will contribute to loads in all six balance components. For this case, force components should be corrected before conversion to coefficient form by

$$\mathbf{F} = \mathbf{F}' - (P_b - P)\begin{bmatrix} S_{bX} \\ S_{bY} \\ S_{bZ} \end{bmatrix} \tag{4.21}$$

where $\mathbf{F}'$ are the uncorrected force components derived from balance outputs and S_{bX}, S_{bY} and S_{bZ} are the projected areas of the base in the x_B', y_B' and z_B' directions respectively.

Similarly the three moment components should be corrected before conversion to coefficient form by

$$\mathbf{G} = \mathbf{G}' - (P_b - P)\begin{bmatrix} 0 & z_c & y_c \\ z_c & 0 & x_c \\ y_c & x_c & 0 \end{bmatrix}\begin{bmatrix} S_{bX} \\ S_{bY} \\ S_{bZ} \end{bmatrix} \tag{4.22}$$

where $\mathbf{G}'$ are the uncorrected moment components derived from balance outputs and x_c, y_c, z_c is the position of the centroid of the base area in the balance axes system.

If, as may occur in some special model mounting arrangements, there is more than one base area, then the above analysis should be carried out for each, and the effects summed.

Where hinge moments are measured on a model, it is customary to express them by coefficients of the form

$$C_H = \frac{h}{q\, S_H\, d_H} \tag{4.23}$$

where h is the measured hinge moment and S_H and d_H are a characteristic area and length associated with the control surface.

4.6 *Transformation to Body Axes*

Aerodynamic coefficients considered thus far have been expressed in balance axes. The transformation to express the coefficients in body axes must take into account not only the possible rotational misalignment of the two axes systems but also the non-coincidence of their origins.

Consider first the rotational misalignment. The transformation matrix which rotates the balance axes into the body axes may be best expressed in terms of three readily measured angles defined as:

ξ_1 –the angle between the projection of the model x_B-axis in the $x_B'y_B'$ plane and the x_B'-axis – positive nose to starboard.

ξ_2—the angle between the model x_B-axis and its projection on the $x_B'y_B'$ plane—positive nose up.

ξ_3—the angle between the model z_B-axis and its projection in the $x_B'z_B'$ plane—positive clockwise looking forward.

Note that this set of angles is not a set of Euler angles—each rotation is about the undisturbed axis. This set of angles is chosen however to make measurement of the required angles as simple as possible. In terms of these angles it may be shown that the transformation matrix is given by

$$[\lambda]_{BB'} =$$

$$\begin{bmatrix} \cos\xi_1\cos\xi_2 & \sin\xi_1\cos\xi_2 & -\sin\xi_2 \\ \dfrac{\sin\xi_2\sin\xi_3 - A\cos\xi_1\sin\xi_2\cos^2\xi_2}{B} & A & \dfrac{\cos\xi_2(\cos\xi_1\sin\xi_3 + A\sin\xi_1\sin\xi_2)}{B} \\ \dfrac{\cos\xi_1\sin\xi_1\cos^2\xi_2\sin\xi_3 + A\sin\xi_2}{B} & -\sin\xi_3 & \dfrac{\cos\xi_2(-\sin\xi_1\sin\xi_2\sin\xi_3 + A\cos\xi_1)}{B} \end{bmatrix} \quad \ldots (4.24)$$

where

$$A = \sqrt{\cos^2\xi_3 \quad \sin^2\xi_1\cos^2\xi_2}$$

and

$$B = \cos^2\xi_1\cos^2\xi_2 + \sin^2\xi_2$$

Hence the transformation of the force coefficients is given by

$$\mathbf{F}_B = [\lambda]_{BB'}\,\mathbf{F}_{B'} \tag{4.25}$$

The transformation of each component of the moment must also include the contribution from a possible shift in origin between the two axes systems, and may be expressed as

$$\mathbf{G}_B = [\lambda]_{BB'}\,\mathbf{G}_{B'} + \begin{bmatrix} 0 & \dfrac{z_b}{b} & \dfrac{y_b}{b} \\ \dfrac{z_b}{c} & 0 & \dfrac{x_b}{c} \\ \dfrac{y_b}{b} & \dfrac{x_b}{b} & 0 \end{bmatrix} \mathbf{F}_B \tag{4.26}$$

where (x_b, y_b, z_b) is the location of the origin of the body axes system with respect to the origin of the balance axes system, b is the reference length used to non-dimensionalize rolling- and yawing-moment coefficients, and c the reference length used to non-dimensionalize the pitching moment coefficient. Note that since the rotations are applied first, followed by the translation, x_b, y_b, z_b must be measured in body (i.e. model) axes rather than balance axes.

5. DETERMINATION OF MODEL ATTITUDE

Application of the processes described in the previous section results in a set of model aerodynamic load coefficients expressed in the body-axes system. Before these coefficients may be transferred to other axes systems, the aerodynamic angles α and β defining the direction of the relative motion between the model and the wind vector must be determined. This in turn requires that the model orientation angles ψ, θ and ϕ be known.

Practical wind tunnel model support rigs usually only allow two of the three orientation angles to be controlled. The two most popular arrangements are the yaw–pitch (ψ, θ) rig and the pitch–roll (θ, ϕ) rig. In the former, the model is yawed through an angle ψ about the z_B' axis and then pitched through an angle θ about the rotated y_B' axis. In the latter case, the model is pitched through an angle θ about the y_B' axis and then rolled through an angle ϕ about the rotated x_B' axis. In both cases the rotations may be considered as sub-sets of the general rotations through all three angles (ψ, θ, ϕ).

In the past several years, several systems have been proposed for measuring the orientation angles directly.[10,11,12] Most of these systems use optical sensors of some type. However, until such systems are in general use, current, less satisfactory approaches must be used. If the model is large enough, the preferred approach is to mount three accelerometers inside the model to measure the components of the gravity vector in three orthogonal directions. If the model is not large enough to accept the accelerometer package (approximately 75 mm cube), the orientation angles must be computed from a knowledge of the attitude of the sting root (i.e. that set by the model support rig). In this case, it is clear that any deflection of the balance and or sting must be taken into account. Although not as obvious, balance and or sting deflections must also be taken into account when the aerodynamic angles are computed from the outputs of a set of tri-axial accelerometers.

Finally, in obtaining the orientation angles (which are measured relative to the tunnel axis system), it is clear that any angular offsets between the measuring systems in use and the tunnel axes system must be included.

5.1 Calculation of Model Deflections

Differences between the orientation angles and the angles set by the model support rig will in general be due to deflections in all parts of the mechanism attaching the model to "earth". It is useful to divide the complete mechanism into two distinct parts when considering deflections. One part, including the balance and the portion of sting upstream of any roll angle producing mechanism, is ammenable to a general analysis. In many cases, this part of the mechanism can be removed and its deflection characteristics measured experimentally. The remainder of the mechanism cannot be easily characterised in a general manner.

For the removable (balance sting) part of the mechanism, it will be assumed that deflection angles are small enough that the deflection remains elastic, allowing the deflection angles to be described simply by a linear stiffness times a load. Hence the angular deflections may be represented as functions of the absolute applied loads by

$$\begin{bmatrix} \upsilon \\ \eta \\ \chi \end{bmatrix} \quad [K]\,\mathbf{H}_B' \tag{5.1}$$

where υ, η and χ are the (small) angular deflections about the balance axes x_B', y_B' and z_B' respectively, $[K]$ is a 3×6 matrix of stiffness, and $\mathbf{H}_B'$ are the absolute loads applied to the balance. Note that since $\mathbf{H}_B'$ are absolute loads, including contributions from both aerodynamics and gravity, no iteration is necessary to determine the angular deflections (as would be the case if non-absolute loads were used).

For many practical balance/sting arrangements, many of the 36 stiffness terms in $[K]$ will be zero. For example, if the balance/sting neutral axes are coincident with the balance axes (i.e. a fully symmetric arrangement), then $[K]$ will have the form

$$[K] = \begin{bmatrix} 0 & 0 & 0 & k_1 & 0 & 0 \\ 0 & 0 & 0 & 0 & k_2 & 0 \\ 0 & 0 & 0 & 0 & 0 & k_3 \end{bmatrix} \tag{5.2}$$

If, as is common, the neutral axes coincide with the x_B' and y_B' axes but not the z_B' axis, two extra terms will appear in $[K]$ thus

$$[K] = \begin{bmatrix} 0 & 0 & 0 & k_1 & 0 & 0 \\ 0 & 0 & k_2 & 0 & k_3 & 0 \\ 0 & k_4 & 0 & 0 & 0 & k_5 \end{bmatrix} \tag{5.3}$$

The deflection angles computed from (5.1) will be expressed in the balance-axes system, and must be transformed to the body-axes system before being used in the calculation of the aerodynamic angles. The simplest way to achieve this transformation is to rewrite (5.1) as

$$\begin{bmatrix} \upsilon \\ \eta \\ \chi \end{bmatrix} = [K]\,\mathbf{H}_B \tag{5.4}$$

where $\mathbf{H}_B$ is obtained from

$$\mathbf{H}_B = [\lambda]_{BB'}\,\mathbf{H}_{B'} \tag{5.5}$$

where $[\lambda]_{BB'}$ is the transformation matrix from balance to body axes presented in (4.24).

Deflection of the part of the model support mechanism between the "earth" end of the balance/sting and earth depends on the physical layout, and hence a general procedure for their treatment is not possible. In most if not all cases, this part of the support will have been designed to be much stiffer than the balance/sting (for which the physical constraints preclude a stiff design), and hence its contribution to the overall deflection of the model can usually be ignored. Those cases for which this assumption is not valid must be considered on an individual basis keeping in mind that some parts of the mechanism may move while others remain fixed when setting up a particular model attitude. Deflections from all parts of the mechanism must be resolved into balance axes (and then to body axes) for each attitude.

5.2 Model Attitude from Sting Root Attitude

The values of yaw, pitch and roll angles indicated by the model support rig readouts must be corrected for angular offsets between the support rig zero datums and the tunnel axes system

$$\left.\begin{aligned} \psi &= \psi_R + \psi_o \\ \theta &= \theta_R + \theta_o \\ \phi &= \phi_R + \phi_o \end{aligned}\right\} \tag{5.6}$$

where ψ_R, θ_R and ϕ_R are the values indicated by the support rig sensors and ψ_o, θ_o and ϕ_o are angular offsets from the tunnel axes to the support rig zero datums. In the absence of significant deflections in the non-removable part of the support rig, these angles represent the attitude of the sting root. With the addition of the angular deflections of the balance and sting (χ, η, υ) computed by the method of the previous section, the aerodynamic angles α and β may be readily calculated. Appendix A sets out the required formulae ((A.10) and (A.12)) and their development. It should be noted that the final forms of these formulae presented in Appendix A are valid only while the angular deflections remain small (less than about $\pm 2^\circ$ if the desired accuracy in α and β is $\pm 0{\cdot}01^\circ$). This will be the case for almost all practical sting/balance combinations. For other cases, a more detailed analysis will be required.

5.3 Model Attitude from Accelerometer Outputs

The output of a set of tri-axial accelerometers mounted in the model is the unit gravity vector

$$\mathbf{g}_A = \begin{bmatrix} \zeta_{XA} \\ \zeta_{YA} \\ \zeta_{ZA} \end{bmatrix} \tag{5.7}$$

whose components ζ_{XA}, ζ_{YA} and ζ_{ZA} are the measured components of the unit gravity vector in the axes system of the accelerometer mounting block (x_A, y_A, z_A). It is worth noting that since $\mathbf{g}_A$ is a unit vector then

$$\zeta_{XA}^2+\zeta_{YA}^2+\zeta_{ZA}^2 = 1 \tag{5.8}$$

In general, the axes system of the accelerometer mounting block will not coincide with the body-axes system. Therefore, to be useful in determining the model attitude, the accelerometer outputs must first be transformed to the body axes system by

$$\mathbf{g}_B = \begin{bmatrix} \zeta_{XB} \\ \zeta_{YB} \\ \zeta_{ZB} \end{bmatrix} = [\lambda]_{BA}\,\mathbf{g}_A \tag{5.9}$$

The transformation matrix $[\lambda]_{BA}$ which rotates the accelerometer mounting block axes into the body axes is best expressed in terms of three readily measured angles (which are analogous to those used to transform the balance axes to body axes) defined by

ω_1—the angle between the projection of the model x_B-axis in the x_Ay_A plane and the x_A axis—positive to starboard.

ω_2—the angle between the model x_B-axis and its projection on the x_Ay_A plane—positive nose up.

ω_3—the angle between the model z_B-axis and its projection in the x_Az_A plane—positive clockwise looking forward.

The transformation matrix $[\lambda]_{BA}$ is then given by equation (4.23) with (ξ_1, ξ_2, ξ_3) replaced by $(\omega_1, \omega_2, \omega_3)$. Again it should be noted that $(\omega_1, \omega_2, \omega_3)$ is not a set of Euler angles. The angles $(\omega_1, \omega_2, \omega_3)$ can be simply determined by measuring the attitude of the model body-axes system with respect to the tunnel-axes system when, with the wind off, the output of the accelerometers is given by

$$\begin{bmatrix} \zeta_{XA} \\ \zeta_{YA} \\ \zeta_{ZA} \end{bmatrix} = \begin{bmatrix} 0 \\ 0 \\ 1 \end{bmatrix} \tag{5.10}$$

i.e. when the accelerometer axes are aligned with the gravity axes.

The pitch and roll angles of the body-axes system will then be given by

$$\theta = \arcsin(\zeta_{XB}) + \theta_0 \tag{5.11}$$

$$\phi = \arctan\left(\frac{\zeta_{YB}}{\zeta_{ZB}}\right) \tag{5.12}$$

where θ_0 is the angular offset between the tunnel free stream velocity vector and the horizontal plane.

For the large pitch angles ($\theta > \pi/4$) it will be more accurate to determine the pitch angle from

$$\theta = \arccos \sqrt{\zeta_{YB}^2 + \zeta_{ZB}^2} + \theta_0 \tag{5.13}$$

It should also be noted that as the pitch angle approaches $\pi/2$, the ζ_{YB} and ζ_{ZB} axes approach the horizontal plane and changes in roll angle will no longer produce changes in the orientations of these accelerometers with respect to the gravity vector. Hence as the pitch angle approaches $\pi/2$, all roll angle information is inevitably lost, and the accuracy of the roll angles derived from (5.12) as the pitch angle approaches $\pi/2$ will be significantly degraded. For a particular test where these limitations are important, it is of course possible to change the orientation of the accelerometer package, or to add extra accelerometers to ensure an accurate determination of roll angle.

Although these values of pitch and roll angles include the effects of the deflection of the support rig, the accelerometer package is insensitive to rotations in the horizontal plane, and hence to any such rotation produced by support rig deflection. This rotation, which for non-zero roll angles will include contributions from angular deflections about both the rotated z_B-axis and the rotated y_B-axis, may be evaluated to sufficient accuracy (so long as angular deflections remain small) from the angular deflections calculated by the methods of section 5.1 by

$$\tan \psi^* = \frac{\sin(\chi \cos\phi - \eta \sin\phi)}{\cos\theta \cos(\chi \cos\phi - \eta \sin\phi)} \tag{5.14}$$

where θ and ϕ are those determined from the accelerometer package. The yaw angle of the body-axes system will then be given by

$$\psi = \psi_R + \psi^* + \psi_0 \tag{5.15}$$

where ψ_R is the yaw angle indicated by the support rig sensor and ψ_0 is the angular offset between the support rig yaw angle datum and the y_T-axis.

The aerodynamic angles α and β may now be calculated from ψ, θ and ϕ using equation (A.1).

6. CORRECTIONS FOR THE EFFECT OF WIND-TUNNEL WALL INTERFERENCE

The measurement of vehicle characteristics from wind tunnel tests, especially at transonic speeds, is subject to several sources of experimental error. One of the most significant of these is wind tunnel wall interference. This section addresses the problem of correcting experimental data for the effects of wind tunnel wall interference.

When a model is placed in a wind tunnel, the aerodynamic loads measured on it differ from those which would be measured if the model were tested under similar conditions in free air, because the wind tunnel walls interfere with the flow around the model. It is usual to make corrections to measured quantities, and to Mach number and model attitude, so that the corrected results correspond to those which would be obtained if the model were tested in free air at the corrected Mach number and attitude. The magnitude of these corrections may be reduced to arbitrarily small values by using models which are small when compared to the test section. However, in an effort to make maximum possible use of the available unit Reynolds number, and hence to minimize errors due to scale effects, models are generally designed with a size which requires significant corrections for the effects of wind tunnel wall interference.

For a model of reasonable size (compared to the test section), these corrections may be calculated from linearized potential flow theory.[13] Changes in local stream direction and stream curvature caused by the presence of the wind tunnel walls preventing the normal flow curvature over a lifting body that occurs in free air, are referred to as lift interference. Changes in local stream velocity and longitudinal gradients caused by the lateral constraint of the flow past the model are referred to as blockage interference. The two types of interference are assumed to be mutually independent.

This classical approach to estimating the effects of wind tunnel wall interference suffers from inaccuracy due to its first order linearized approach and the necessarily simple way in which the physical model is mathematically represented. Despite these limitations, for tests in tunnels with solid walls, the results produced are sufficiently accurate for most development testing. The results for tests in transonic tunnels, which are usually equipped with ventilated (either porous or slotted) walls, are however far from satisfactory. The problem here is one of correctly representing the boundary conditions at the tunnel walls. In the case of solid walls, the boundary conditions are straightforward and mathematically amenable. For ventilated walls, the wall boundary conditions are complex, and it is usual to change the mixed (open, closed) boundary conditions into an equivalent homogeneious one, which produces the same solution at the centre of the test section, but the correct representation remains open to question.[14,15] In most cases, recourse must be made to experiment to determine the correct wall boundary conditions for each particular test section.

In recent years it has been realized that the classical homogenious boundary conditions for ventilated walls is not satisfactory, and further that classical linear theory itself is not adequate to describe the truly non-linear nature of flows at supercritical speeds. In view of the fact that the boundary conditions at the wall are not well defined and are in fact model dependent (through the pressure and flow fields imposed at the wall), the use of measured wall pressure data to infer the wall constraints would appear to be a logical approach. Many proposals to make use of wall pressure data in computing interference corrections have therefore been put forward. The most promising of these also take advantage of advances in our ability to compute transonic flows, to combine a truly non-linear calculation method with measured wall pressure distributions. Such methods are now fairly well developed for the two-dimensional aerofoil case,[16,17] but their routine application to the testing of three-dimensional models is still some way off.[18] Until that time, the estimation of wall interference effects in ventilated test sections must rely on the questionable methods of classical theory.

6.1 Transformation to Wind Axes

Classical linear interference theory has been developed to make use of measured forces and moments expressed in the wind-axes system. Hence before applying any interference corrections, forces and moments must be transformed from the body-axes system to the wind-axes system via

$$\mathbf{F}_W = [\lambda]_{WB}\,\mathbf{F}_B \tag{6.1}$$

and

$$\mathbf{G}_W = [\lambda]_{WB}\,\mathbf{G}_B \tag{6.2}$$

where $[\lambda]_{WB}$ is the required transformation matrix. The required matrix is presented in Appendix B in terms of all common combinations of the aerodynamic angles α_s, β_s, α_t and β_t.

6.2 Application of Classical Theory in Solid-Wall Tunnels

For tunnels with solid walls, the wall boundary conditions are well defined and, at least for subcritical flows, the results of classical interference theory may be used for correcting experimental measurements.

Consider first the corrections which must be made for the lateral constraint of the flow past the model due to the presence of the walls, i.e. the blockage corrections. This effect is equivalent to an increase in the free stream velocity in the vicinity of the model, and for models of normal size, may be considered constant over the model. Hence the corrected free stream velocity is given by

$$V_t = V_t(1+\epsilon) \tag{6.3}$$

where ϵ, the blockage factor, is usually split into separate contributions from the body and from its wake

$$\epsilon = \epsilon_s + \epsilon_w \tag{6.4}$$

For a three-dimensional aircraft model, the contribution from the body, the solid body blockage, ϵ_s, can be further split into contributions from the wing and from the fuselage

$$\epsilon_s = \epsilon_{sb} + \epsilon_{sw} \tag{6.5}$$

According to classical theory, the contribution from the wing may be represented by

$$\epsilon_{sw} = \frac{T}{C^{3/2}}\frac{1}{\beta^3}\left\{1 + 1\cdot 2\beta\left(\frac{t}{c}\right)\right\}V_w \tag{6.6}$$

where C is the tunnel cross-sectional area, V_w is the volume of the wing and T is a constant which depends on the tunnel cross-sectional shape (B/H) and the ratio of wing span to tunnel width (b/B). For a streamlined body of revolution, with length to diameter ratio f, the solid body blockage is given by

$$\epsilon_{sb} = \frac{T}{C^{3/2}}\frac{1}{\beta^3}\left(1 + \frac{0\cdot 4\beta}{f}\right)V_b \tag{6.7}$$

where V_b is the volume of the body.

The contribution of the wake to the blockage factor is given by

$$\epsilon_w = \frac{S}{4C}\frac{1+0\cdot 4M_t^2}{\beta^2}C_{D_0} \tag{6.8}$$

where S is the wing area and M_t the (uncorrected) free stream Mach number, and C_{D_0} is the model zero-lift drag coefficient.

With contributions to the blockage factor ϵ calculated from (6.6), (6.7) and (6.8), free stream quantities may now be corrected by (for $\gamma = 1\cdot 4$):

$$q_f = \{1 + (2 - M_t^2)\epsilon\} q_t \tag{6.9}$$

$$\rho_f = \{1 - M_t^2 \epsilon\} \rho_t \tag{6.10}$$

$$M_f = \{1 + (1 + 0{\cdot}2 M_t^2)\epsilon\} M_t \tag{6.11}$$

$$Re_f = \{1 + (1 - 0{\cdot}7 M_t^2)\epsilon\} Re_t \tag{6.12}$$

Note that classical thoery makes no allowance for bluff body (i.e. stalled wing) blockage. This contribution will be significant in the post-stall region where it may produce an additional correction to dynamic pressure on the order of 1 %.

Turning now to lift interference. The presence of the upper and lower wind tunnel walls modifies the flow curvature over a lifting body that occurs in free air. Corrections must therefore be made to the angle of incidence and to measured coefficients for the mean value and streamwise variation of the induced upwash. By choosing the location of the vortex used by classical theory to represent the circulation to be at the centre of the wing (i.e. mid chord), all the upwash corrections may be included in corrections to the angle of incidence, there being no correction needed for lift coefficient. There remains, however, a residual correction to pitching moment coefficient.

The correction to angle of incidence will in this case be given by

$$\alpha_f = \alpha_t + \frac{S}{C} C_{L,t} \left(\delta_0 + \frac{\lambda c}{2\beta H} \delta_1 \right) \tag{6.13}$$

where δ_0 is related to the mean value of the induced upwash, and δ_1 to the streamwise gradient i.e. to streamline curvature. Note the relative increase in importance of the streamline curvature term with increasing Mach number (decreasing β). It has been usual (especially in low-speed tunnel work) to express equation (6.13) in the form

$$\alpha_f = \alpha_t + \delta_0 \frac{S}{C} C_{L,t} \left(1 + \tau_2 \right) \tag{6.14}$$

δ_0 is then a function only of tunnel shape and may be determined either experimentally or theoretically for a particular tunnel. The constant τ_2 on the other hand is a function of both model and tunnel geometry (and Mach number).

The residual correction to pitching moment coefficient is given by

$$C_{mf} = C_{mt} + \frac{(\Delta\alpha)_{sc}}{8} a \tag{6.15}$$

where a is the wing lift-curve slope, and $(\Delta\alpha)_{sc}$ is the streamline curvature induced correction to angle of incidence which, from equation (6.13) is given by

$$(\Delta\alpha)_{sc} = \frac{\lambda c}{2\beta H} \delta_1 \frac{S}{C} C_{L,t} \tag{6.16}$$

or from equation (6.14)

$$(\Delta\alpha)_{sc} = \tau_2 \delta_0 \frac{S}{C} C_{L,t} \tag{6.17}$$

The upwash induced by the tunnel walls also has the effect of reducing the measured drag due to the wing appearing to have a higher aspect ratio. According to classical theory the correction to drag coefficient is given by

$$C_{Df} = C_{Dt} + \delta_0 \frac{S}{C} C_{L,t}^2 \tag{6.18}$$

Similarly the induced upwash will influence the flow field of any tailplane which must also be corrected. The correction to the tailplane angle takes the form of equations (6.13) or (6.14) with $C/2$ replaced by l_T (the distance of the tailplane aerodynamic centre aft of the aerodynamic centre of the wing) in (6.13) and with τ_2 evaluated at the tailplane location in (6.14).

An additional correction is required to the drag coefficient because the images of the source representing the wake impose a longitudinal pressure gradient along the tunnel and hence a longitudinal bouyancy force on the model. This pressure gradient may conveniently be regarded as linear along the length of the model. This correction will then be given by

$$\Delta C_D = C_{Dt}\,(1+0{\cdot}4M_t^2)\,\epsilon_s \tag{6.19}$$

The total correction to drag coefficient for the effects of both lift and blockage interference and for longitudinal bouyancy therefore becomes

$$C_{Df} = \left\{C_{Dt} + \delta_0 \frac{S}{C} C_{Lt}^2 + (1+0{\cdot}4M_t^2)C_{Dt}\right\} \Big/ \left\{1+(2-M_t^2)\,\epsilon\right\} \tag{6.20}$$

and the total correction to pitching moment coefficient becomes

$$C_{mf} = \left\{C_{mf} + a\frac{(\Delta\alpha)_{sc}}{8}\right\} \Big/ \left\{1+(2-M_t^2)\,\epsilon\right\} \tag{6.21}$$

For all other coefficients, the only correction required is that due to blockage so that *lift* coefficient, for example, becomes

$$C_{Lf} = C_{Lt}/\{1+(2-M_t^2)\epsilon\} \tag{6.22}$$

The results from classical interference theory quoted above are not valid in the most general case. Several simplifying assumptions have been made as follows:

(i) It has been assumed that the model and specifically the centre of pressure of the wing remain on the tunnel centre line. Movements off the centre line will require modifications to both the lift interference factors δ_0 and δ_1 and the solid blockage factor ϵ_s.

(ii) No account has been taken of effects due to asymmetric wing loading with the model symmetric in the tunnel nor to asymmetric placement of the model in the tunnel (both due to rolling and yawing of the model).

(iii) No account has been taken of possible bouyancy effects (affecting drag coefficient) due to a variation of the empty tunnel longitudinal pressure along the test section axis.

In general these assumptions produce small errors, within the expected accuracy of classical theory. All of these effects can however be included in the structure of the theory, and if any of the above assumptions are severely violated, the magnitude of the error should be investigated and included if significant.

6.3 Application of Classical Theory in Ventilated-Wall Tunnels

In principle, the walls of a ventilated wall tunnel affect the flow over a model in a similar manner to those of a tunnel with open or closed walls. Since many interference parameters change sign between the open and closed wall cases, it is theoretically possible to design ventilated walls which reduce or eliminate some sources of interference. However, in practice ventilated walls are often arranged primarily for the generation of low supersonic Mach numbers using

diffuser suction, or to minimize shock reflections at high subsonic and low supersonic Mach numbers, with little attempt made to utilize the available cancellation of interference.

The application of classical interference theory to wind tunnels with ventilated walls makes use of the same set of relationships as presented for solid-wall tunnels in the previous section, but with differing values of the parameters ϵ, δ_0 and δ_1. The approach of linear interference theory to calculating these parameters is to represent the ventilated walls by an equivalent homogenious boundary conditions characterised (for slotted walls) by two wall parameters. The first of these, the slot parameter F, is a function of the geometry of the slotted wall given by

$$F = \frac{2d}{\pi H} \ln \left\{ \operatorname{cosec} \frac{\pi a}{2d} \right\} \tag{6.23}$$

where d is the periodic spacing of the slots whose width is a. F is supposed to represent the effect of the slot geometry on the tunnel centre line. Equation (6.23) is a very simple representation, taking no account of the finite thickness of the slots, or the separation on the plenum side of the slot. Many more complex expressions (see for example Refs 14 and 15) have been proposed to better represent the slot geometry.

The second parameter characterising the slotted wall, the porosity parameter P (or more usually β. P), is also used to characterise the porous wall. It is introduced in the slotted wall case to take account of viscous effects in the slots, and is analogous to the term expressing the linearized pressure drop across a porous wall. Unlike F, there is no way of computing β. P *a priori*, but the effects of viscosity on the flow through a slot are obviously important, especially when the slot width is on the same order as the wall boundary layer thickness. It is doubtful however, even if β. P correctly characterizes the outflow of working section fluid, whether a simple linear parameter can ever hope to characterize the inflow of fluid from the plenum chamber. In this case it is possible that the fluid entering the slots could be more or less stagnant. The situation is further complicated by the influence of the model on the growth of tunnel wall boundary layers, in which case it becomes doubtful whether a single value of β/P could be valid for all tests with particular walls, or even the whole of one wall for a particular test.

Given these problems, it is not surprising that classical linear theory is much less successful in predicting interference in ventilated wall tunnels than in solid wall tunnels. Even for the mathematically simpler case of the two-dimensional aerofoil, experiments[19] confirm the basic failure of linear theory to correctly predict interference effects. For three-dimensional testing the results are even less satisfactory. Hence it has been the practice at A.R.L. not to correct results obtained in ventilated (slotted) walls for interference. This approach is justified on the basis of the following:

(i) Ventilated walls are used only for testing at high (transonic) speeds for which other considerations encourage the use of models which are smaller (when compared to test section area) than are generally used at low speeds, reducing the magnitude of the interference effects.

(ii) The ventilated walls in use in A.R.L. tunnels, although not designed to eliminate interference, do produce significantly smaller interference than do solid walls.

(iii) The probable inaccuracies in linear interference theory for ventilated walls are expected to be on the same order as the total interference corrections.

6.4 Transformation to Other Axes Systems

It is not unusual for wind tunnel test customers to request that data be presented in an axes system other than the wind-axes system. Hence once interference corrections have been applied the data must be transformed back to the body-axes and or stability-axes system. This transformation is achieved via the application of a suitable transformation matrix, for example from wind-axes to stability-axes via

$$\mathbf{F} = [\lambda]_{SW}\,\mathbf{F}_W$$

and

$$\mathbf{G}_S = [\lambda]_{SW}\,\mathbf{G}_W$$

Transformation matrices to transform data between body, stability and wind axes are presented in Appendix B in terms of all common combinations of the aerodynamic angles α_s, β_s, α_t and β_t

7. CONCLUSIONS

This report has presented a general approach to the reduction and processing of wind tunnel data. It has not attempted to provide a general approach for all possible types of wind tunnel testing, but has concentrated on procedures applicable to force and moment data acquired from internal sting mounted strain gauge balances. The procedures should however be applicable, with minor variations, to force and moment data acquired from modern load-cell based external balances. Although every attemp has been made to keep the approach as general as possible within its area of application, not all possibilities have been included. For example, the practice, found necessary at some wind tunnels, of using separate strain gauge balance calibration factors for each sign of applied load, has not been considered. This practice has so far been found to be unnecessary with the types of balance in use at A.R.L. Such decisions have also been made in several other areas. Overall, the procedures as presented are sufficiently general to include all those effects which have been found necessary for the types of tests and balances so far encountered in A.R.L. wind tunnels.

Finally, it is worth noting once again, that no matter how general (and hopefully accurate) the computer representations of the algorithms included in a data acquisition system may be, the final results will only be as accurate as the least accurate information used in the reduction process. Thus, no matter how good the data acquisition system, an inaccurate balance calibration matrix for example, will ensure inaccurate results. The often quoted adage concerning computer processing — garbage in, garbage out — has never been more appropriate.

ACKNOWLEDGEMENTS

This work is based on an approach to the reduction of internal strain gauge balance data developed at A.R.L. over the past 25 years. Of the many people who have made significant contributions to this development, the author would particularly wish to record the contributions of Messrs J. B. Willis, D. A. Secomb, N. Pollock and the late Dr I. A. Hunt.

REFERENCES

1. Secomb, D. A. Notes on the Computer Programme for Force Measurements in the Transonic Wind Tunnel. A.R.L. Tech. Memo. 192, 1964.

2. Palko, R. L., and Lohr, A. D. A Constant Parameter Testing Technique with Automatic Wind Tunnel Control. A.I.A.A. Paper No. 78-784, 1979.

3. Fairlie, B. D. A Real-Time Data Acquisition System for a Low-Speed Wind Tunnel. A.R.L. Aero. Report 163, 1985.

4. Warren, C. H. E. The Definition of the Angles of Incidence and Sideslip. RAE Tech. Note Aero. 2187, 1952.

5. Jaeger, L. G. Cartesian Tensors in Engineering Science. Pergamon, 1966.

6. Pollock, N. A Simple High Performance Device for Measuring Strain Gauge Transducer Outputs. J. Phys. E., Scientific Insts., 8, 1049, 1975.

7. Cook, T. A. A Note on the Calibration of Strain Gauge Balances for Wind Tunnel Models. RAE Tech. Note Aero. 2631, 1954.

8. Smith, D. L. An Efficient Algorithm using Matrix Methods to Solve Wind Tunnel Force Balance Equations. NASA TN-D-6860 1972.

9. Galway, R. D. A Comparison of Methods for Calibration and Use of Multi-Component Strain Gauge Wind Tunnel Balances. N.R.C. Aero Report LR-600, 1980.

10. Pond, C. R., and Texeira P. D. Laser Angle Sensor Development. NASA CR-159385 1980.

11. Goethert, W. H. A Direct Model Pitch Measurement with a Laser Interferometer Using Retroreflectors. AEDC TR-79-87 1980.

12. Law, R. D., and Tuck, A. N. System for the Measurement of the Attitude of Wind Tunnel Models. RAE Tech. Memo. Aero. 1834, 1980.

13. Garner, H. C., Rodgers, E. W. E., Acum, W. E. A., and Maskell, E. C. Subsonic Wind-Tunnel Wall Corrections. AGARDograph 109, 1966.

14. Berndt, S. B., and Sörensen, H. Flow Properties of Slotted Walls for Transonic Test Sections. AGARD CP-174, 1976.

15. Woods, L. C. On the Theory of Two-Dimensional Wind Tunnels with Slotted Walls. Proc. Roy. Soc. A, 233, 74, 1955.

16. Kemp, W. B. Transonic Assessment of Two-Dimensional Wind-Tunnel Wall Interference Using Measured Wall Pressures. NASA CP-2045, 1978.

17. Mokry, M., and Ohman, L. H. Application of the Fast Fourier Transforms to Two-Dimensional Wind-Tunnel Wall Interference. J. Aircraft, 17, 402, 1980.

18. Farris, R. C., and Jacocks, J. L. Prediction of Transonic Wind-Tunnel Wall Interference. AEDC TR-83-48, 1983.

19. Fairlie, B. D., and Pollock, N. Evaluation of Wall Interference Effects in a Two-Dimensional Transonic Wind Tunnel by Subsonic Linear Theory. A.R.L. Aero. Report 151, 1979.

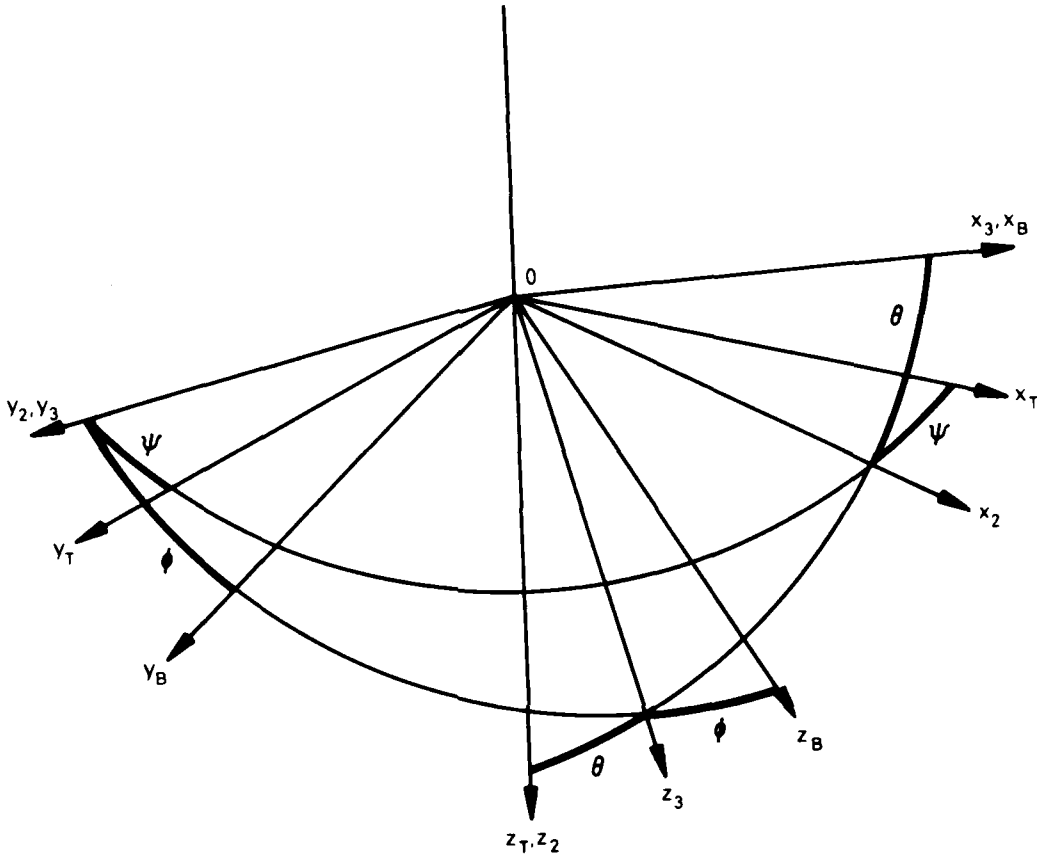

FIG. 1 EULER ANGLES

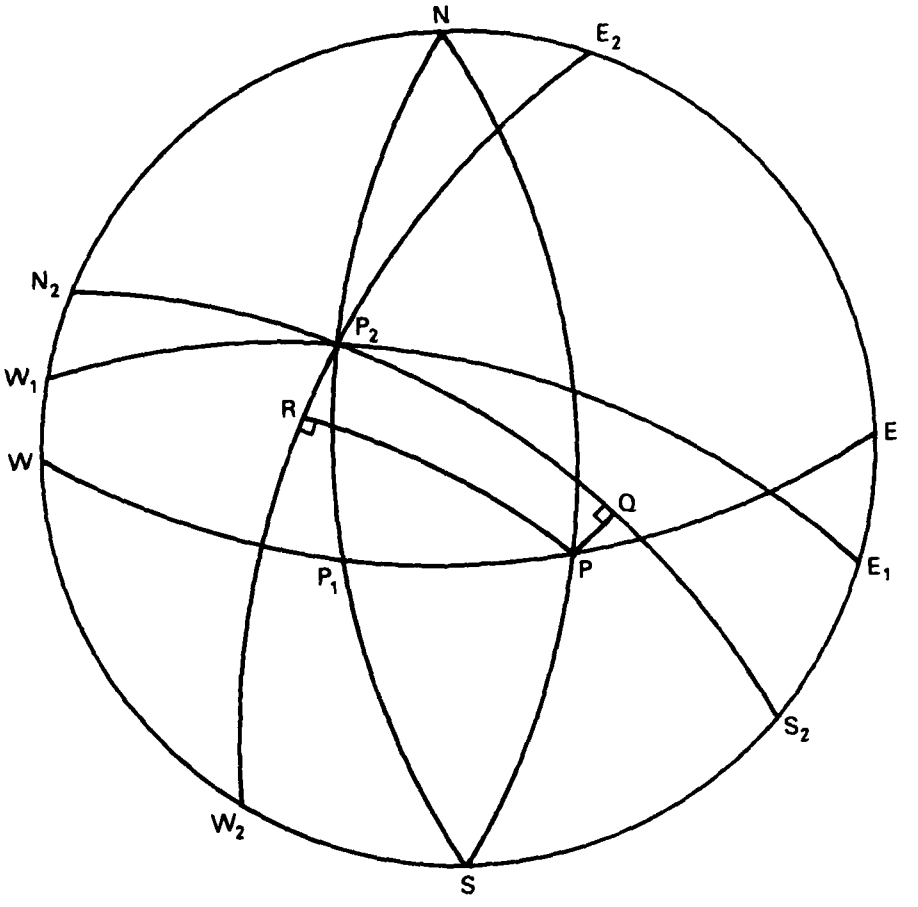

FIG. 2 DEFINITION OF AERODYNAMIC ANGLES

APPENDIX A

Relationships Between Aerodynamic and Orientation Angles

When a wind tunnel model is set up at some attitude, the set of Euler angles (ψ, θ, ϕ) through which the model is rotated to reach that altitude may be related to the aerodynamic angles α and β by

$$\left.\begin{aligned} \sin \alpha_s &= \cos \psi \sin \theta \cos \phi + \sin \psi \sin \phi \\ \sin \beta_s &= \cos \psi \sin \theta \sin \phi - \sin \psi \cos \phi \\ \tan \alpha_t &= \tan \theta \cos \phi + \frac{\tan \psi \sin \phi}{\cos \theta} \\ \tan \beta_t &= \tan \theta \sin \phi - \frac{\tan \psi \cos \phi}{\cos \theta} \end{aligned}\right\} \quad (A.1)$$

It should be noted that the order of the rotations (ψ, θ, ϕ) is significant. If another of the six possible rotation orders is used, then the above relationships no longer hold. For example, if the rotations are applied in the order (θ, ϕ, ψ), then the above relationships become

$$\left.\begin{aligned} \sin \alpha_s &= \sin \theta \cos \phi \\ \sin \beta_s &= \sin \theta \sin \phi \cos \psi - \cos \theta \sin \psi \\ \tan \alpha_t &= \frac{\tan \theta \cos \phi}{\cos \psi + \tan \theta \sin \phi \sin \psi} \\ \tan \beta_t &= \frac{\tan \theta \sin \phi - \tan \psi}{1 + \tan \theta \sin \phi \tan \psi} \end{aligned}\right\} \quad (A.2)$$

In most wind tunnels, model support mechanisms are capable of providing only a subset of the full (ψ, θ, ϕ) set of Euler rotations. The most commonly available rigs are the pitch/roll (θ, ϕ) rig, and the yaw/pitch rig (ψ, θ). Such rigs produce the subset of Euler rotations in the same order as the full set. In such cases the general relationships (A.1) simplify considerably. For the pitch/roll (θ, ϕ) rig they become

$$\left.\begin{aligned} \sin \alpha_s &= \sin \theta \cos \phi \\ \sin \beta_s &= \sin \theta \sin \phi \\ \tan \alpha_t &= \tan \theta \cos \phi \\ \tan \beta_t &= \tan \theta \sin \phi \end{aligned}\right\} \quad (A.3)$$

and for the yaw/pitch (ψ, θ) rig

$$\left.\begin{aligned} \sin \alpha_s &= \sin \theta \cos \psi \\ \sin \beta_s &= -\sin \psi \\ \tan \alpha_t &= \tan \theta \\ \tan \beta_t &= -\tan \psi / \cos \theta \end{aligned}\right\} \quad \text{(A.4)}$$

The last set explain the reason for the popularity of α_t and β_s as the choice of aerodynamic angles in low-speed wind tunnels (where model rigs are traditionally of the yaw/pitch type), for in this case

$$\left.\begin{aligned} \beta_s &= -\psi \\ \alpha_t &= \theta \end{aligned}\right\} \quad \text{(A.5)}$$

As well as allowing the use of the above simplified relationships the limitation to two Euler rotations also makes available some particularly simple inverse relationships. These are, for the pitch/roll (θ ϕ) rig

$$\left.\begin{aligned} \cos \theta &= \cos \alpha_t \cos \beta_s \\ \tan \phi &= \tan \beta_s / \sin \alpha_t \\ \sin^2 \theta &= \sin^2 \alpha_s + \sin^2 \beta_s \\ \tan \phi &= \sin \beta_s / \sin \alpha_s \\ \tan^2 \theta &= \tan^2 \alpha_t + \tan^2 \beta_t \\ \tan \phi &= \tan \beta_t / \tan \alpha_t \end{aligned}\right\} \quad \text{(A.6)}$$

and for the yaw/pitch (ψ θ) rig

$$\left.\begin{aligned} \theta &= \alpha_t \\ \psi &= -\beta_s \\ \sin \theta &= \sin \alpha_s / \cos \beta_s \\ \psi &= -\beta_s \\ \theta &= \alpha_t \\ \tan \psi &= -\tan \beta_t / \cos \alpha_t \end{aligned}\right\} \quad \text{(A.7)}$$

Note that the above inverse relationships are grouped into three pairs of equations for θ and ϕ or ψ and θ, one pair for each possible choice of pairs of aerodynamic angles — (α_t, β_s), (α_s, β_s) or (α_t, β_t). It is apparent that for the pitch/roll rig, the above expressions introduce an ambiguity in the correct sign of θ. However, if the roll angle is in the range $-\pi/2 < \phi \leq \pi/2$ (a range which, when combined with pitch angles in the range $-\pi/2 < \theta \leq \pi/2$, gives access to all values of α and β) then the correct sign of θ is the same as that of α (either α_s or α_t). Similar inverse relationships cannot be derived for the general (ψ, θ, ϕ) case since in that case any given combination of aerodynamic angles can be produced by an infinite number of combinations of the three orientation angles.

The relationships presented thus far should be interpreted as relating the aerodynamic angles and the orientation angles of the sting root, that is the orientation angles as set by the model support rig. In practice the sting and balance will deflect under the applied loads (both gravitational and aerodynamic) and the orientation angles of the body-axes system will differ from those of the sting root. Unless model attitude is measured via on-board accelerometers, these deflections must be taken into account when calculating the aerodynamic angles. (See Section 5 for the effect of deflections on accelerometer measured attitudes). The effect of deflections on the relationship between aerodynamic and orientation angles for both the pitch/roll rig and the yaw/pitch rig are presented below. In the derivation of these relationships it has been assumed that the deflections are small, and hence that the order of application of the rotations is not significant. Hence the order of application chosen for each case is that which results in the simplest relationships. However, it is worth noting that the relationships are exact for the set of Euler rotations applied in the stated order.

Consider first a pitch/roll rig (θ, ϕ) for which the deflections of the balance and sting are given by

χ—deflection in the yaw direction — i.e. a rotation about the $0z$ axis.

η—deflection in the pitch direction — i.e. a rotation about the $0y$ axis.

υ—deflection in the roll direction — i.e. a rotation about the $0x$ axis.

Then for deflections applied in the order (υ, η, χ), the aerodynamic angles are given by

$$\left.\begin{aligned}
\sin\alpha_s &= \sin\theta\cos\phi'\cos\eta+\cos\theta\sin\eta \\
\sin\beta_s &= \sin\theta\sin\phi'\cos\chi-\sin\chi\,(\cos\theta\cos\eta-\sin\theta\sin\eta) \\
\tan\alpha_t &= \frac{\sin\theta\cos\phi'\cos\eta+\cos\theta\sin\eta}{\cos\chi\,(\cos\theta\cos\eta-\sin\theta\cos\phi'\sin\eta)+\sin\theta\sin\phi'\sin\chi} \\
\tan\beta_t &= \frac{\sin\theta\sin\phi'\cos\chi-\sin\chi\,(\cos\theta\cos\eta-\sin\theta\sin\eta)}{\cos\chi\,(\cos\theta\cos\eta-\sin\theta\cos\phi'\sin\eta)+\sin\theta\sin\phi'\sin\chi} \\
\text{where}\quad \phi' &= \phi+\upsilon
\end{aligned}\right\} \qquad (A.8)$$

In most cases, the deflections are small enough that the approximations

$$\left.\begin{aligned}
&\cos\chi=\cos\eta=\cos\upsilon\approx 1 \\
&\sin\chi\approx\chi\,;\quad \sin\eta\approx\eta\,;\quad \sin\upsilon\approx\upsilon
\end{aligned}\right\} \qquad (A.9)$$

can be made and (A.8) can be reduced to

$$\left.\begin{aligned}
\sin\alpha_s &= \sin\theta\cos\phi'+\eta\cos\theta \\
\sin\beta_s &= \sin\theta\sin\phi'-\chi\cos\theta \\
\tan\alpha_t &= \frac{\tan\theta\cos\phi'+\eta}{1+\tan\theta\,(\chi\sin\phi'+\eta\cos\phi')} \\
\tan\beta_t &= \frac{\tan\theta\sin\phi'-\chi}{1+\tan\theta\,(\chi\sin\phi'-\eta\cos\phi')} \\
\phi' &= \phi+\upsilon
\end{aligned}\right\} \qquad (A.10)$$

For a yaw/pitch (ψ, θ) rig, applying the same deflections, but in the order (η, υ, ψ) gives

$$\left.\begin{aligned}
\sin \alpha_s &= \cos \psi \sin \phi' \cos \upsilon + \sin \psi \sin \upsilon \\
\sin \beta_s &= -\sin \psi \cos \upsilon \cos \chi - \cos \psi \cos \phi' \sin \chi + \cos \psi \sin \phi' \sin \upsilon \cos \chi \\
\tan \alpha_t &= \frac{\sin \theta' \cos \upsilon + \tan \psi \sin \upsilon}{\cos \theta' \cos \chi + \sin \theta' \sin \upsilon \sin \chi - \tan \psi \cos \upsilon \sin \chi} \\
\tan \beta_t &= \frac{-\tan \psi \cos \upsilon \cos \chi - \cos \theta' \sin \chi + \sin \theta' \sin \upsilon \cos \chi}{\cos \theta' \cos \chi + \sin \theta' \sin \upsilon \sin \chi - \tan \psi \cos \upsilon \sin \chi}
\end{aligned}\right\} \quad \text{(A.11)}$$

where $\theta' = \theta + \eta$

Once again, if the approximations of (A.9) are valid, these relationships reduce to

$$\left.\begin{aligned}
\sin \alpha_s &= \cos \psi \sin \theta' + \upsilon \sin \psi \\
\sin \beta_s &= -\sin \psi - \chi \cos \psi \cos \theta' + \upsilon \cos \psi \sin \theta' \\
\tan \alpha_t &= \frac{\sin \theta' + \upsilon \tan \psi}{\cos \theta' - \chi \tan \psi} \\
\tan \beta_t &= \frac{-\tan \psi - \chi \cos \theta' + \upsilon \sin \theta'}{\cos \theta' - \chi \tan \psi}
\end{aligned}\right\} \quad \text{(A.12)}$$

where $\theta' = \theta + \eta$

APPENDIX B

Axes Transformations

This Appendix presents a collection of transformation matrices for the transformation of vectors between the body-axes system and both the stability- and wind-axes systems. Transformations are given in terms of the matrix $[\lambda]_{12}$ where the components of a vector **A** in axes-system 1 are rotated to those in axes-system 2 by

$$\begin{bmatrix} A_{X1} \\ A_{Y1} \\ A_{Z1} \end{bmatrix} = [\lambda]_{12} \begin{bmatrix} A_{X2} \\ A_{Y2} \\ A_{Z2} \end{bmatrix}$$

or

$$\mathbf{A}_1 = [\lambda]_{12}\, \mathbf{A}_2$$

The matrix $[\lambda]_{12}$ is given in terms of all the useful combinations of the aerodynamic angles α_s, β_s, α_t and β_t.

B1.—Transformations in Terms of α_t, β_s.

From body axes to stability axes.

$$[\lambda]_{SB} = \begin{bmatrix} \cos\alpha_t & 0 & \sin\alpha_t \\ 0 & 1 & 0 \\ -\sin\alpha_t & 0 & \cos\alpha_t \end{bmatrix}$$

From body axes to wind axes:

$$[\lambda]_{WB} = \begin{bmatrix} \cos\alpha_t\cos\beta_s & \sin\beta_s & \sin\alpha_t\cos\beta_s \\ -\cos\alpha_t\sin\beta_s & \cos\beta_s & -\sin\alpha_t\sin\beta_s \\ -\sin\alpha_t & 0 & \cos\alpha_t \end{bmatrix}$$

B2.—Transformations in Terms of α_s, β_s.

From body axes to stability axes:

$$[\lambda]_{SB} = \begin{bmatrix} \sec\beta_s\sqrt{\cos^2\alpha_s - \sin^2\beta_s} & 0 & \sin\alpha_s\sec\beta_s \\ 0 & 1 & 0 \\ -\sin\alpha_s\sec\beta_s & 0 & \sec\beta_s\sqrt{\cos^2\alpha_s - \sin^2\beta_s} \end{bmatrix}$$

From body axes to wind axes:

$$[\lambda]_{WB} = \begin{bmatrix} \sqrt{\cos^2\alpha_s - \sin^2\beta_s} & \sin\beta_s & \sin\alpha_s \\ -\tan\beta_s\sqrt{\cos^2\alpha_s - \sin^2\beta_s} & \cos\beta_s & -\sin\alpha_s\tan\beta_s \\ -\sin\alpha_s\sec\beta_s & 0 & \sec\beta_s\sqrt{\cos^2\alpha_s - \sin^2\beta_s} \end{bmatrix}$$

B3.—Transformations in Terms of α_t, β_t.

From body axes to stability axes:

$$[\lambda]_{SB} = \begin{bmatrix} \cos\alpha_t & 0 & \sin\alpha_t \\ 0 & 1 & 0 \\ -\sin\alpha_t & 0 & \cos\alpha_t \end{bmatrix}$$

From body axes to wind axes:

$$[\lambda]_{WB} \begin{bmatrix} \dfrac{1}{\sqrt{\sec^2\alpha_t + \tan^2\beta_t}} & \dfrac{\tan\beta_t}{\sqrt{\sec^2\alpha_t + \tan^2\beta_t}} & \dfrac{\tan\alpha_t}{\sqrt{\sec^2\alpha_t + \tan^2\beta_t}} \\ \dfrac{\cos\alpha_t\tan\beta_t}{\sqrt{\sec^2\alpha_t + \tan^2\beta_t}} & \dfrac{\sec\alpha_t}{\sqrt{\sec^2\alpha_t + \tan^2\beta_t}} & \dfrac{-\sin\alpha_t\tan\beta_t}{\sqrt{\sec^2\alpha_t + \tan^2\beta_t}} \\ \sin\alpha_t & 0 & \cos\alpha_t \end{bmatrix}$$

B4.—Inverse Transformations.

There is no need to list the inverse transformations, e.g. from wind axes to body axes — $[\lambda]_{BW}$, since

$$[\lambda]_{BW} = [\lambda]_{WB}^{-1}$$

and making use of the property of direction cosines that

$$[\lambda]^{-1} = [\lambda]^{T}$$

then

$$[\lambda]_{BW} = [\lambda]_{WB}{}^{T}$$

i.e. the inverse of a transformation is obtained by simply taking the transpose of the direct matrix.

B5.—Transformations Between Other Systems.

Transformations between the stability- and wind-axes systems may be derived from the matrices listed above as follows. We wish to find the matrix $[\lambda]_{SW}$ such that

$$\mathbf{A}_S = [\lambda]_{SW}\,\mathbf{A}_W$$

Now

$$\mathbf{A}_W = [\lambda]_{WB}\,\mathbf{A}_B$$

Hence

$$\mathbf{A}_S = [\lambda]_{SW}\,[\lambda]_{WB}\,\mathbf{A}_B$$

But we also know that

$$\mathbf{A}_S = [\lambda]_{SB}\,\mathbf{A}_B$$

Hence

$$[\lambda]_{SW}\,[\lambda]_{WB} = [\lambda]_{SB}$$

i.e.

$$[\lambda]_{SW} = [\lambda]_{SB}\,[\lambda]_{WB}{}^{-1}$$

$$= [\lambda]_{SB}\,[\lambda]_{WB}{}^{T}$$

Hence in terms of α_t and β_s (the most useful pair for this transformation)

$$[\lambda]_{SW} = \begin{bmatrix} \cos\beta & \sin\beta & 0 \\ \sin\beta & \cos\beta & 0 \\ 0 & 0 & 1 \end{bmatrix}$$

Similar transformations for other α, β pairs may be derived from the matrices listed above.

DISTRIBUTION

AUSTRALIA

DEPARTMENT OF DEFENCE

Central Office

Chief Defence Scientist
Deputy Chief Defence Scientist
Superintendent, Science and Program Administration
Controller, External Relations, Projects and Analytical Studies
(1 copy)
Defence Science Adviser (UK) (Doc. Data sheet only)
Counsellor, Defence Science (USA) (Doc. Data sheet only)
Defence Science Representative (Bangkok)
Defence Central Library
Document Exchange Centre, DISB (18 copies)
Joint Intelligence Organisation
Librarian H Block, Victoria Barracks, Melbourne

Aeronautical Research Laboratories

Director
Library
Superintendent—Aerodynamics
Divisional File—Aerodynamics
Author: B. Fairlie
M. A. Balicki
K. A. O'Dwyer
M. K. Glaister
J. F. Harvey
J. N. Hodges
N. Pollock
C. W. Sutton
J. Wattmuff

Materials Research Laboratories

Director/Library

Defence Research Centre

Library

Air Force Office

Air Force Scientific Adviser
Aircraft Research and Development Unit
Scientific Flight Group
Library

Technical Division Library
Director General Aircraft Engineering—Air Force
RAAF Academy, Point Cook

Government Aircraft Factories
Manager
Library

STATUTORY AND STATE AUTHORITIES AND INDUSTRY
Australian Aircraft Consortium Pty. Ltd.
Mr D. Pilkington
Mr R. D. Bullen
Commonwealth Aircraft Corporation, Library
Hawker de Havilland Aust. Pty. Ltd., Bankstown, Library

UNIVERSITIES AND COLLEGES

Adelaide	Barr Smith Library
	Professor of Mechanical Engineering
Flinders	Library
La Trobe	Library
Melbourne	Engineering Library
Monash	Hargrave Library
Newcastle	Library
Sydney	Engineering Library
NSW	Physical Sciences Library
Queensland	Library
Tasmania	Engineering Library
Western Australia	Library
RMIT	Library
	Dr P. H. Hoffman, Aero. Engineering

CANADA
NRC
Aeronautical & Mechanical Engineering Library

FRANCE
ONERA, Library

INDIA
Defence Ministry, Aero Development Establishment, Library
National Aeronautical Laboratory, Information Centre

JAPAN
Institute of Space and Astronautical Science, Library

NETHERLANDS

National Aerospace Laboratory (NLR), Library

NEW ZEALAND

RNZAF, Vice Consul (Defence Liaison)
Transport Ministry, Airworthiness Branch, Library

SWEDEN

Aeronautical Research Institute, Library

UNITED KINGDOM

CAARC, Secretary
Royal Aircraft Establishment
Bedford, Library
British Library, Lending Division
Aircraft Research Association, Library
Motor Industry Research Association, Director

Universities and Colleges

Bristol	Engineering Library
Cambridge	Library, Engineering Department
	Whittle Library
Nottingham	Science Library
Southampton	Library
Cranfield Institute of Technology	Library
Imperial College	Aeronautics Library

UNITED STATES OF AMERICA

NASA Scientific and Technical Information Facility

SPARES (20 copies)

TOTAL (106 copies)

Department of Defence

DOCUMENT CONTROL DATA

1. a. AR No.	1. b. Establishment No.	2. Document Date	3. Task No.
AR-004-017	ARL-AERO-R-164	May, 1984	DST 82/022

4. Title	5. Security	6. No. Pages
ALGORITHMS FOR THE REDUCTION OF WIND-TUNNEL DATA DERIVED FROM STRAIN-GAUGE FORCE BALANCES	a. document: Unclassified b. title: U. c. abstract: U.	44 7. No. Refs: 19

8. Author(s)	9. Downgrading Instructions
B. D. Fairlie	

10. Corporate Author and Address	11. Authority (*as appropriate*)
Aeronautical Research Laboratories P.O. Box 4331, Melbourne, Vic., 3001	a. Sponsor b. Security c. Downgrading d. Approval

12. Secondary Distribution (*of this document*)

Approved for public release.

Overseas enquirers outside stated limitations should be referred through ASDIS, Defence Information Services Branch, Department of Defence, Campbell Park, CANBERRA, ACT, 2601.

13. a. This document may be ANNOUNCED in catalogues and awareness services available to . . .

No limitations.

13. b. Citation for other purposes (*i.e. casual announcement*) may be (*select*) unrestricted (*or*) as for 13 a.

14. Descriptors	15. COSATI Group
Algorithms Data reduction Wind tunnel apparatus Loads (forces) Moments	01010 14020

16. Abstract

Algorithms and procedures are presented for the reduction of force and moment data derived from wind-tunnel models supported by internal strain-gauge balances. The algorithms are developed in their most general forms, suitable for implementation on the new generation of powerful minicomputers currently being included in wind-tunnel data acquisition systems. Although the emphasis of the report is on the treatment of data derived from sting mounted strain-gauge force balances, the analysis is applicable, with only minor modifications, to data derived from modern load-cell based external force balances.

This page is to be used to record information which is required by the Establishment for its own use but which will not be added to the DISTIS data base unless specifically requested.

16. Abstract (Contd)		
17. Imprint *Aeronautical Research Laboratories, Melbourne*		
18. Document Series and Number Aerodynamic Report 164	19. Cost Code 54-6060	20. *Type of Report and Period Covered*
21. Computer Programs Used —		
22. Establishment File Ref(s) —		

END

DATE
FILMED

2-86

DTIC